THE EFFECTS OF PROTON BOMBARDMENT ON PbSnTe

David Graham Anderson

NAVAL POSTGRADUATE SCHOOL

Monterey, California

THESIS

THE EFFECTS OF PROTON BOMBARDMENT ON PbSnTe

by

David Graham Anderson

Thesis Advisor: T. F. Tao

December 1972

Approved for public release; distribution unlimited.

The Effects of Proton Bombardment
on PbSnTe

by

David Graham Anderson
Lieutenant, United States Navy
B.S., University of Southern California, 1965

Submitted in partial fulfillment of the
requirements for the degree of

MASTER OF SCIENCE IN ELECTRICAL ENGINEERING

from the

NAVAL POSTGRADUATE SCHOOL
December 1972

ABSTRACT

The effects of 200-250 KeV proton bombardment on both p-type and n-type $Pb_{0.80}Sn_{0.20}Te$ thin films were investigated. Emphasis was placed on p-type samples to determine the feasibility and dosage required to change the carrier type and to determine the stability after bombardment. This method of conversion has promise in the fabrication of photovoltaic diode arrays for infrared applications. The samples were characterized by Hall effect and conductivity measurements from 90°K to 300°K. It was found that p-type $Pb_{0.80}Sn_{0.20}Te$ samples of initial concentrations in the low to mid $10^{17}/cm^3$ range can be converted to n-type with dosages above 5×10^{15} p/cm^2, considerably higher than the low to mid 10^{13} p/cm^2 needed to convert $Pb_{1-x}Sn_xTe$ of other Sn contents. Stability was investigated using isochronal annealing methods with temperatures up to 180°C. It was found that significant changes of the proton bombardment effects occurred around 140°C. Type converted n samples were found to return to p-type at this temperature.

TABLE OF CONTENTS

LIST OF TABLES

LIST OF FIGURES

ACKNOWLEDGEMENTS

I would like to first thank Professor Tien-Fan Tao under whose guidance and encouragement this thesis was made possible and Professor Cheng-Chi Wang for his numerous contributions to both the theoretical and experimental aspects of this study. I am also deeply grateful to Mr. Raymond Zahm who prepared the initial samples and provided technical advice on the equipment used, and to Petty Officer Milton Jaehnig for his invaluable help during the electrical measurements portion of this research.

I would also like to thank Mr. Bruce Hauss of U.C.L.A. and Dr. Donald Simons and Mr. Richard Schoolar of the Naval Ordnance Laboratory for their time and special effort in bombarding the samples used. I would like to acknowledge the support of the Air Force Materials Laboratory in this research.

I am especially grateful to my wife, Sharon, for her assistance in typing the rough drafts of this thesis, but most especially, for her support and understanding during the long hours I was unable to spend with her.

My apologies to my sons, Michael and Patrick, who only knew me as the man who came home for dinner and then went back to school, and my hopes that this study may in some small way contribute to a better world for them.

I. INTRODUCTION

A. OBJECTIVE OF THIS RESEARCH

Recently, proton bombardment and ion implantation have generated much interest in the field of semiconductor device fabrication. Proton bombardment and ion implantation have the capability of changing the electrical properties, including carrier concentration and carrier type, in many semiconductor materials. These properties, combined with their ability to make these changes in very well defined lateral and vertical regions with a wide range of concentrations, have created many applications in integrated circuit and optoelectric technologies.

The purpose of this research was to study the effect of proton bombardment on the electrical properties of $Pb_{0.80}Sn_{0.20}Te$. Since it was not intended to make a study of the junction properties of this semiconductor material, thin films were used to ensure that the effects of proton bombardment would be uniform throughout the depth of the sample. Electrical properties were studied using Hall effect and conductivity measurements. The stability of proton bombardment effects were studied using the isochronal annealing method.

$Pb_{1-x}Sn_xTe$ is of interest because its energy gap can be tailored by adjusting the alloy compositions to fall within a broad infrared spectral range. This property allows PbSnTe

to be used in long wavelength infrared applications. Passive applications include infrared imaging. Because of the obvious military applications, Department of Defense agencies have been heavily supporting development of passive infrared detection reconnaissance and surveillance $Pb_{1-x}Sn_xTe$ devices. Active applications include environmental pollution monitors [Ref. 1], laser communications systems and laser detection systems. Using $Pb_{1-x}Sn_xTe$, junction lasers have been made from both vapor and Bridgman grown crystals after proper isothermal annealing [Refs. 2 and 3]. Sensitive photovoltaic detectors for the 8-14 micron wavelength range operating at liquid nitrogen temperatures have also been fabricated from Bridgman and vapor growth crystals [Refs. 4 and 5]. $Pb_{0.80}Sn_{0.20}Te$ is of specific interest because at liquid nitrogen temperature its energy gap corresponds to an infrared wavelength of CO_2 laser systems.

The results of this study will assist the current efforts in developing long wavelength photovoltaic detector arrays using either proton bombardment or ion implantation. Such arrays are the most promising candidates for infrared imaging.

Proton bombardment has been successfully used to fabricate satisfactory PbTe and $Pb_{0.88}Sn_{0.12}Te$ photovoltaic detectors. However, attempts to extend this technique to PbSnTe containing higher Sn contents for long wavelength infrared applications have not been as successful. The type

conversion of p-type $Pb_{1-x}Sn_xTe$ to n-type has not been consistent for Sn contents higher than 12%. Previous research by others in this group has demonstrated that p-type $Pb_{1-x}Sn_xTe$ of 24% can be consistently converted to n-type by moderate proton dosages if the initial carrier concentration is in the low $10^{17}/cm^3$. However, they also found that the same dosage was unable to convert p-type $Pb_{1-x}Sn_xTe$ of 20% Sn. It is to this specific problem that this research addresses itself.

B. THE NATURE OF $Pb_{1-x}Sn_xTe$ NARROW GAP SEMICONDUCTORS

The binary semiconductor $Pb_{1-x}Sn_xTe$ has a composition dependent energy gap which can be made arbitrarily small by changing the alloy composition, x, and temperature, T. By controlling the parameters of composition and temperature, energy gaps of zero to 0.3 ev. are possible (see Figure 1) [Ref. 6]. The model for the energy bands in $Pb_{1-x}Sn_xTe$ was originally proposed by Dimmock et al. [Ref. 7] and inferred from laser emission at low temperatures [Refs. 7 and 8], from optical absorption data at room temperature [Refs. 9 and 10] and from the results of tunneling experiments [Ref. 11]. As a result, it has become the subject of extensive study for long wavelength infrared lasers and detectors.

Lead and tin combine with telluride to form the binary compounds PbTe and SnTe which possess the cubic rock salt or NaCl crystal structure. Single crystals of rock salt structure $Pb_{1-x}Sn_xTe$ have been grown from the melt by the

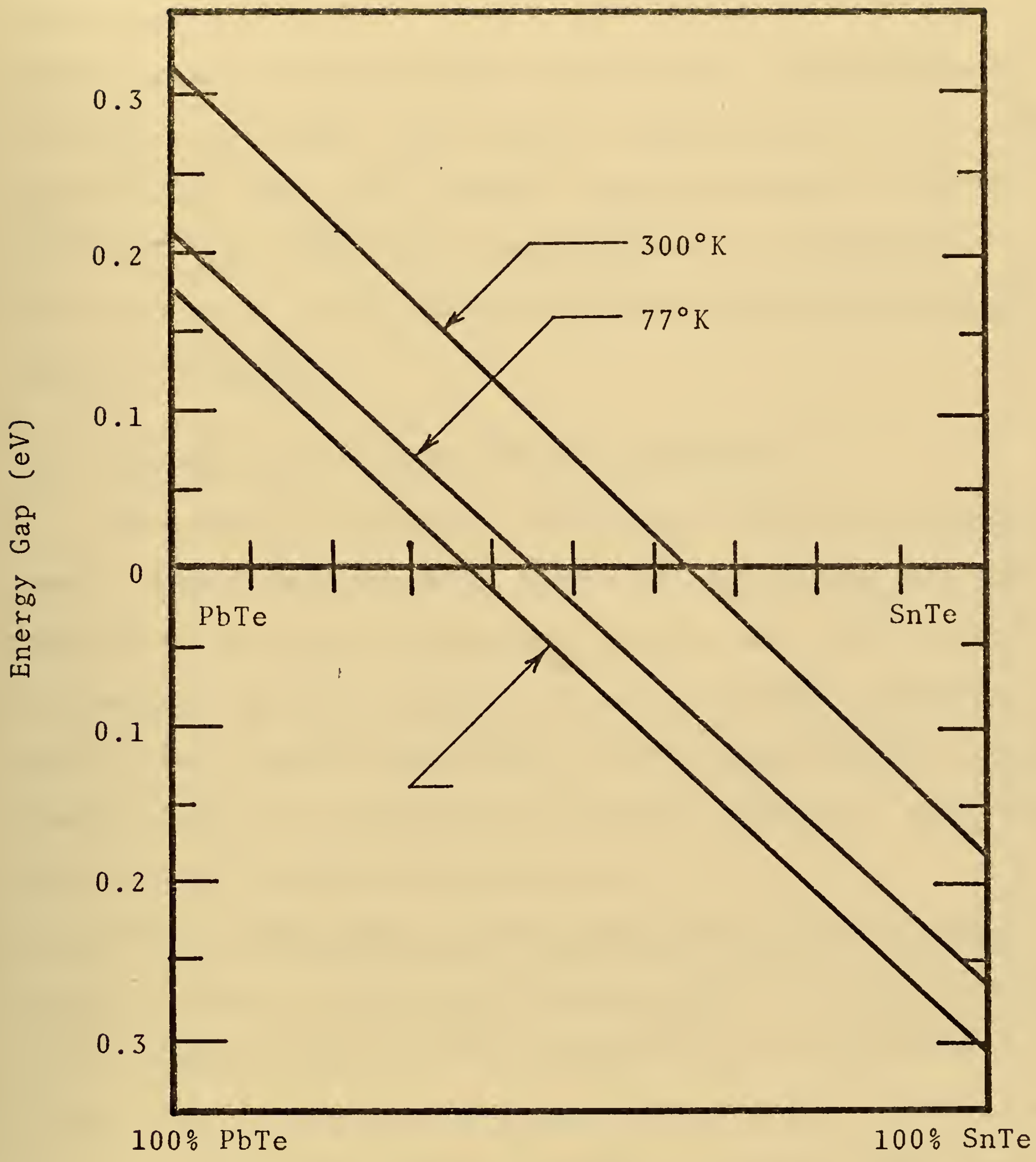

Figure 1

Energy gap of $Pb_{1-x}Sn_xTe$ as a function of x, the mole fraction of SnTe

Bridgman [Ref. 12] and the Czochralski [Ref. 13] techniques, from the vapor in both closed and open [Ref.s 14 and 15] tube growth processes, and from the solution by liquid phase epitaxy process [Refs. 16 and 17]. Although the crystals, as grown, have carrier concentrations in the order of $10^{19}/cm^3$ [Ref. 18], carrier concentrations as low as $10^{15}/cm^3$ [Ref. 18], have been obtained in crystals of $x = 0.17$ to $x = 0.20$ using isothermal annealing processes and/or by doping.

C. ION IMPLANTATION AND PROTON BOMBARDMENT

This thesis research is concerned with proton bombardment. Until very recently [Refs. 19, 20, 21 and 22] the potential of proton bombardment process as a fabrication technique for practical devices was not known. However, much effort has been expended in developing the ion implantation process to fabricate electronic devices. This effort has met with considerable success.

Proton bombardment in some semiconductors has played a role similar to that of ion implantation. In the following, a brief description of ion implantation will be given followed by a description of proton bombardment. In this manner, the advantages and current interest in proton bombardment can be presented in a broader perspective.

1. Ion Implantation

Ion implantation is a relatively new semiconductor processing technique used in conjunction with diffusion

processes to further improve and simplify device fabrication. Implantation techniques have been used to form p-n junctions in silicon, germianium, gallium arsenide, cadmium telluride, silicon carbide and many other semiconductors. There has been recent interest in ion implantation for the fabrication of more sophisticated devices. Presently, high frequency MOS devices [Ref. 23 and 24], depletion and enhancement devices on the same chip [Ref. 25] and IMPATT devices [Ref. 26] are in production using implantation techniques. There is also recent interest in using ion implantation to fabricate buried channel charge coupled devices [Ref. 27].

The advantages of ion implantation are numerous. The number of implanted ions and their depth distributions can be externally controlled by voltage and current. The geometrical control of the implanted area can be achieved by the use of masks (including metal, photoresist or oxide layer), and lateral spreading of the dopant is insignificant. The physical properties of the substrate do not restrict the type of dopant used, giving a wider choice of dopants. Another distinct advantage is that ion implantation is a relatively low temperature process.

The equipment and techniques for ion implantation are straightforward and have been known for about twenty years. It is only recently that insight has been gained into the physical nature of the implanted layer. Ion implantation is not an equilibrium process. As the implanted

ion slows and comes to rest in the substrate it creates a region of heavy disorder along the entry path. Annealing procedures are generally required if the electrical characteristics of the implanted layers are to be determined by the nature of the implanted ions rather than the disorder created by their entry.

The important parameters used in characterizing implantation in semiconductor substrates are the depth distribution of the implanted ions (see Figure 2)[Ref. 26], the amount of lattice disorder, the anneal behavior, the lattice location of the implanted ions and the electrical characteristics of the implanted layer.

Figure 3 [Ref. 26] shows a typical ion implantation system. The ion source, floating at the highest system voltage, generates a plasma which contains the desired dopant. This beam emerges from a lens directly into a multistage acceleration column (acceleration can also take place after mass separation) where it is accelerated to its full potential. A large mass separation magnet separates the desired element from the rest of the beam. Beyond the magnet, deflection plates sweep the beam to make uniform wide-area implants on the target substrate. The target samples are mounted in the temperature controlled target chamber which is essentially at ground potential. Typical implantation beam currents are of the order of one to ten amperes with voltages of 20-300 KeV [Ref. 28].

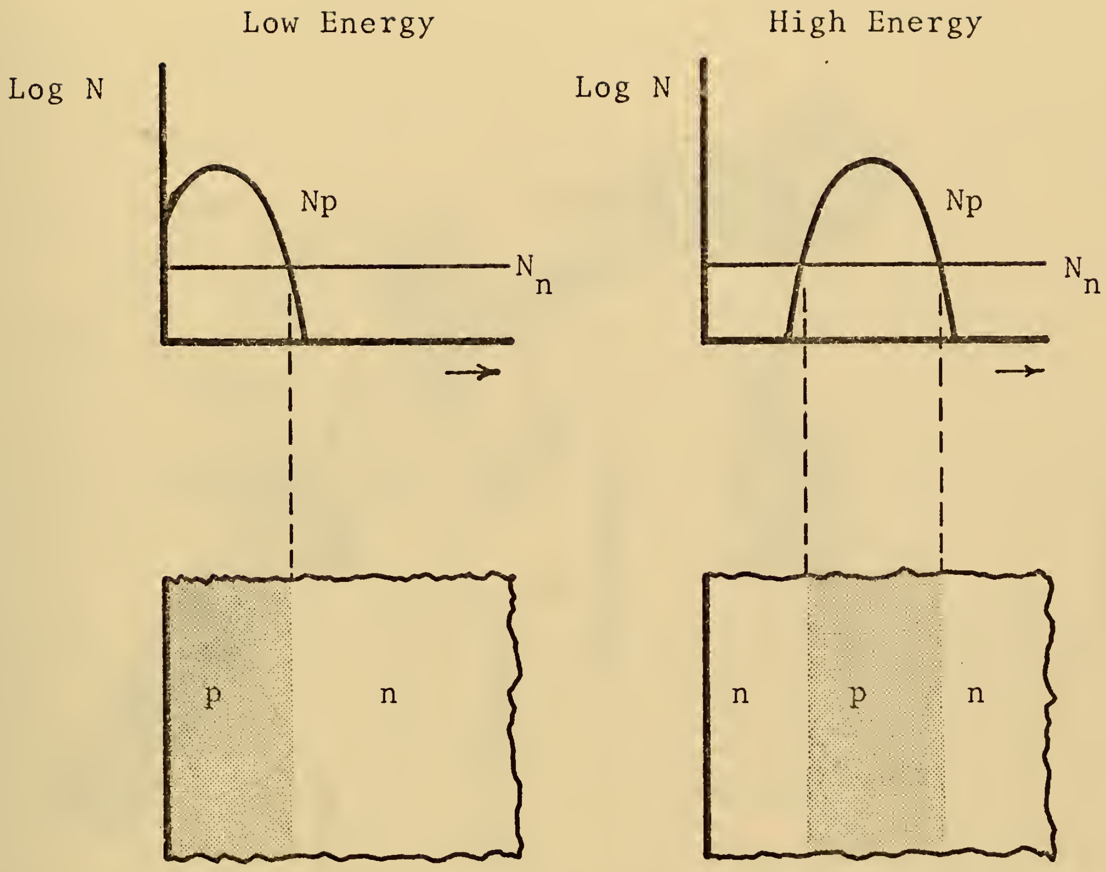

Figure 2

Implanted Junctions. Assuming ideal distribution the amount of energy provides accurate control of the location of the junction or buried layer.

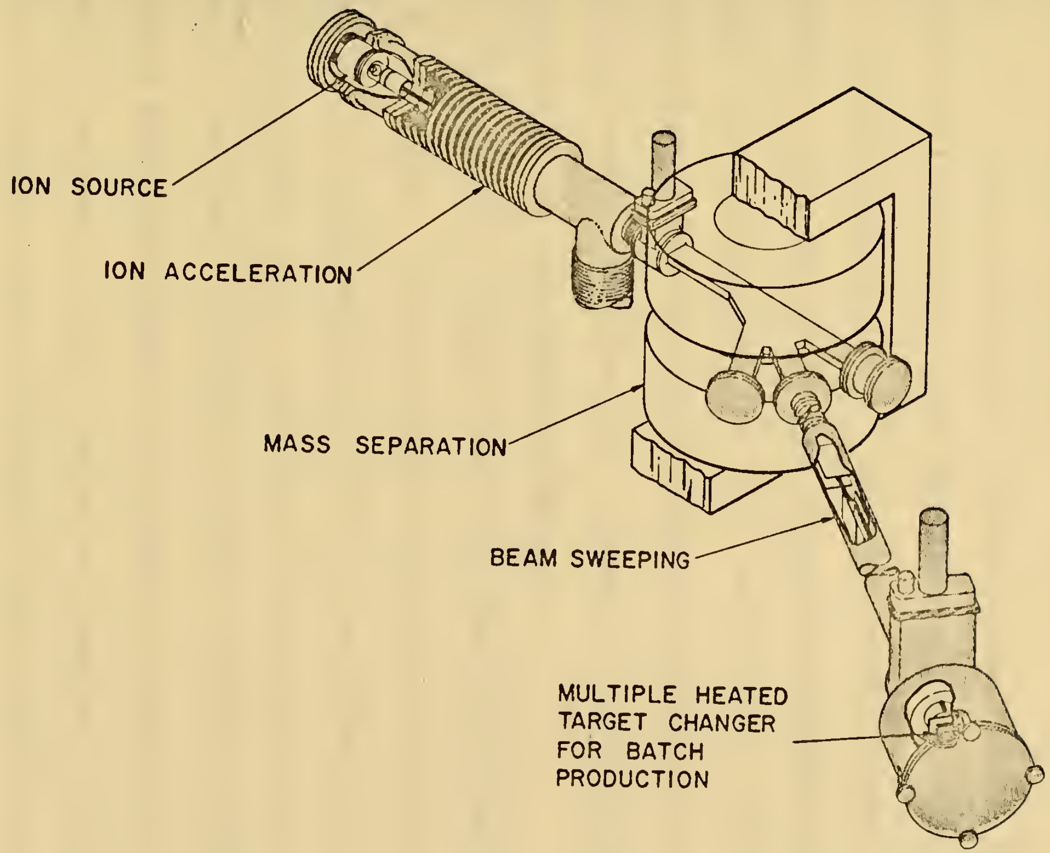

Figure 3

Ion Implantation System with Pre-acceleration

Ion implantation in compound semiconductors has not been fully studied. However, there is growing interest along these lines because of the many possible applications. Donally et al. [Ref. 29] have converted n-type CdTe forming p-n junctions by implanting 400 KeV As^+ ions. Implantation of Group V elements has produced p-type regions on the surface of n-type CdS [Refs. 30 and 31]. It is probable that efficient solar cells can be made from these materials.

Implantation of Sb^+ ions to convert layers of p-type PbTe into n-type material has been accomplished [Ref. 32]. The photodiodes prepared by this method have exhibited zero bias resistance one to two orders of magnitude higher than those previously reported and therefore have higher detectivities in reduced background.

Ion implantation junctions have also been made in both α and β-SiC. The n-type regions have been formed in p-type SiC by implanting 20 KeV Sb ions [Ref. 33] and 400 KeV P ions [Ref. 34]. Junctions in p-type β-SiC have been formed by implanting 30 KeV Al ions. Anneal temperatures as low as 800°C have been successful in activating the implanted regions. This should be compared with the normal diffusion temperatures of greater than 1900°C used in device fabrication for SiC. There is strong indication that blue light emitting diodes (LED's) can be fabricated by ion implantation in SiC.

In GaAs, junction characteristics of good quality have been obtained from implantation of Group II and VI elements [Refs. 35, 36 and 37]. In some cases the diode characteristics exhibit behavior similar to shallow graded p-i-n structures.

2. Proton Bombardment

In some compound and alloy semiconductors where nonstoichiometrics such as vacancies and interstitial ions play important roles in affecting the semiconducting properties, it has been reported that proton bombardment can be used to change their properties. In this fashion, proton bombardment can be considered as a variation of ion implantation. Instead of implanting impurity ions, proton bombardment creates vacancies and/or interstitial ions which are electrically active and behave as donors and acceptors.

It was recently reported that proton bombardment can change the surface layer of several p-type semiconductors to n-type semiconductors. Using this effect, n-p junctions of InSb [Ref. 38], $Hg_{1-x}Cd_xTe$ [Ref. 19], PbTe [Ref. 20], and $Pb_{0.88}Sn_{0.12}Te$ [Ref. 21] have been made. Used as photovoltaic detectors, they were reported to have high zero bias resistance, fast response and high sensitivity.

In GaAs, proton bombardment (or O or Cr implantation) can change semiconducting GaAs into semi-insulating GaAs. It has promising potential in GaAs integrated circuit work.

Recently, proton bombardment has been used to produce continuous wave lasers in PbTe and $Pb_{1-x}Sn_xTe$ [Ref. 22].

3. Annealing and Lattice Disorder

The distribution of ions during implantation is highly dependent upon the structure of the material being bombarded and its orientation. As the ions lose energy and stop in the substrate they undergo violent collisions with the lattice atoms, displacing them from lattice sites. The displaced atoms can in turn displace other atoms. The diameter of the disordered region is on the order of 10-100 Å [Ref. 28]. A major part of this lattice disorder can be restored by proper annealing. If the total number of implanted ions is large (greater than $10^{14}/cm^2$) [Ref. 28] the disordered regions overlap forming an amorphous layer. Annealing to restore lattice structure in this amorphous region generally requires temperatures twice as high as those required to restore disorders. In crystaline substrates, ion "channeling" can occur. If the direction of motion of the incident ion is aligned with a low index crystallographic direction, it will be channeled or steered through the crystal without violent collisions with lattice atoms. Channeled ions will penetrate the substrate 2-50 times deeper than non-channeled ions [Ref. 28]. Because some of the ions will strike lattice atoms, concentrations of greater than $10^{14}/cm^2$ implanted ions will still produce an amorphous layer in the substrate. Complete elimination of channeling is not

possible; however, there are two methods used to reduce channeling. One method presumes a knowledge of crystal orientation. By tilting the crystal off-axis, channeling will be significantly reduced. The second method involves the deliberate formation of an amorphous layer on the substrate to dechannel the ions before they get to the substrate. The amorphous layer can be an oxide layer, or an inert species can be implanted first to create an amorphous layer.

Two types of annealing, isochronal and isothermal, have been used to investigate the nature and stability of bombardment induced defects. Since the characteristics of the narrow gap $Pb_{1-x}Sn_xTe$ semiconductors can only be revealed at low temperatures, isothermal annealing which monitors the electrical properties at the annealing temperature as a function of time, is impractical. This research therefore employs the isochronal annealing method to determine the stability of proton bombardment induced defects.

II. EXPERIMENTAL ASPECTS

A. PREPARATION OF $Pb_{0.80}Sn_{0.20}Te$ THIN FILMS

Thin films of $Pb_{0.80}Sn_{0.20}Te$ used in this research were prepared by a one boat evaporation method [Refs. 10 and 39]. This single source technique yielded more reproducible alloy compositions and controllable crystal structures. The source materials were small chunks of polycrystalline $Pb_{1-x}Sn_xTe$ alloys prepared by melding 99.9999% pure Pb, Sn, and Te with suitable proportions so that the proper composition could be obtained. The substrates were commercially available BaF_2 and CaF_2 single crystals cleaved along (111) planes immediately before deposition.

1. Preparation of Source Materials

Initially, 99.9999% pure Pb, Sn, and Te were weighed on a Sartorius Type 2403 analytic balance to provide suitable proportion for the composition desired. Both the stoichiometric [$(\text{Metal})_{0.50}$ $(\text{Chalcogenide})_{0.50}$] and the metal rich [$(\text{Metal})_{0.52}$ $(\text{Chalcogenide})_{0.48}$] materials were made in the same way. The stoichiometric materials were used for depositions, and the metal rich materials were used for isothermal annealing. For $Pb_{0.80}Sn_{0.20}Te$ the ratios shown below were used.

	Pb	Sn	Te
Stoichiometric	6.9826	1.0000	5.3753
Metal Rich	6.9826	1.0000	5.1646

After the elements had been properly weighed they were placed in a chemically cleaned quartz tube and evacuated using a diffusion vacuum pump system down to a pressure on the order of 10^{-6} torr then sealed. The sealed tube was then placed in a furnace whose temperature was raised gradually to about 100°C above the melting point of the material which is 900°C for $Pb_{0.80}Sn_{0.20}Te$. The tube was left in the furnace for more than 20 hours to ensure thorough mixing of the elements. Afterwards the tube was quenched in water. The polycrystalline stoichiometric ingots were then used as the source material for thin film deposition.

2. Deposition of Thin Films

a. Deposition System

The thin film depositions were carried out in a diffusion pump system equipped with a liquid nitrogen cold trap capable of maintaining a vacuum of the order of 10^{-6} torr during deposition (See Figure 4). The deposition unit is shown in Figures 5 and 6. It was enclosed in a stainless steel enclosure and placed in a pyrex bell jar. The distance between the substrate and heated boat was approximately six inches.

The substrates were mounted in a stainless steel substrate holder which contained seven samples. The substrates were mounted behind masks in order to produce films whose shapes were suitable for Hall or optical measurements. A chromel alumel thermocouple was placed on the surface of

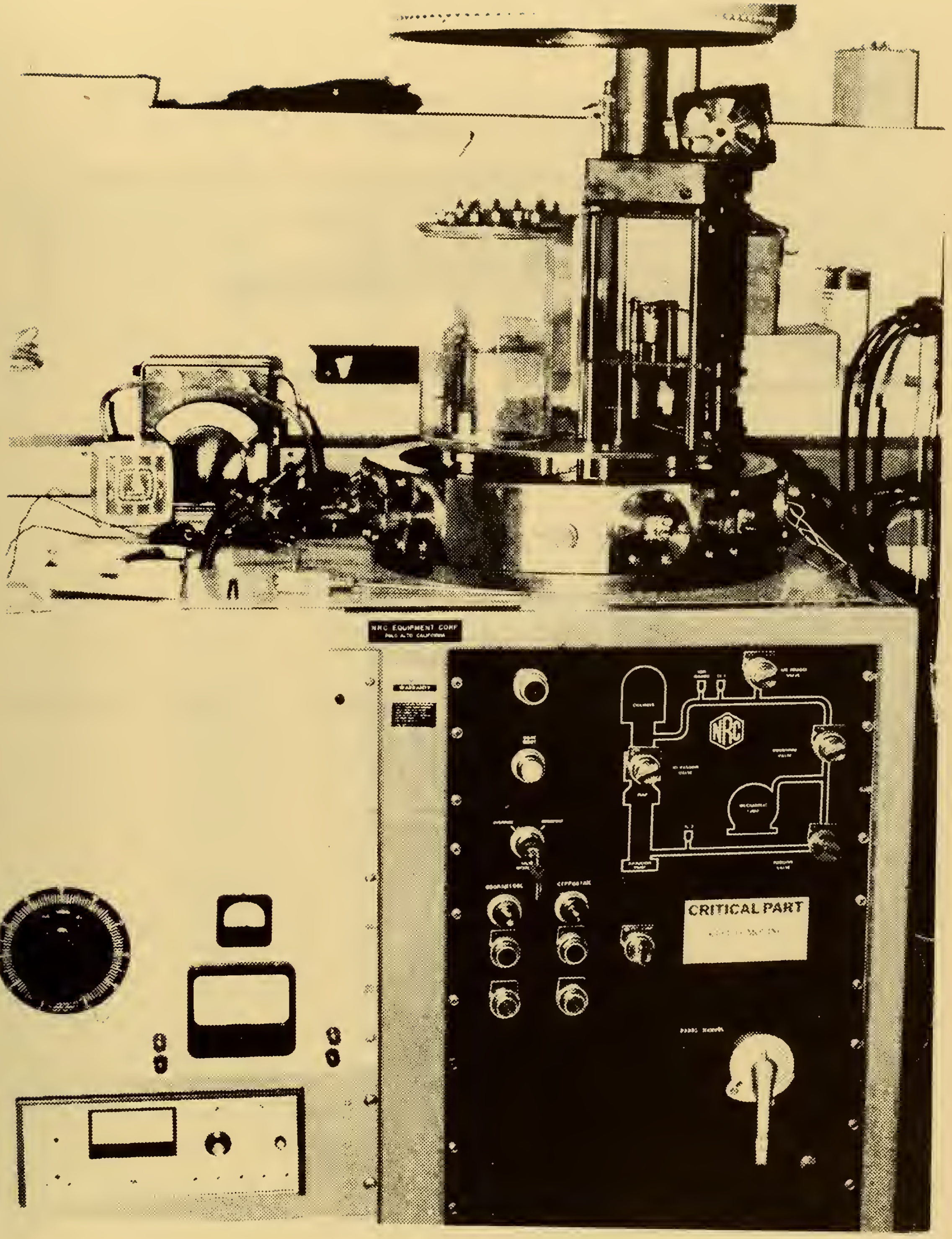

Figure 4
Deposition System

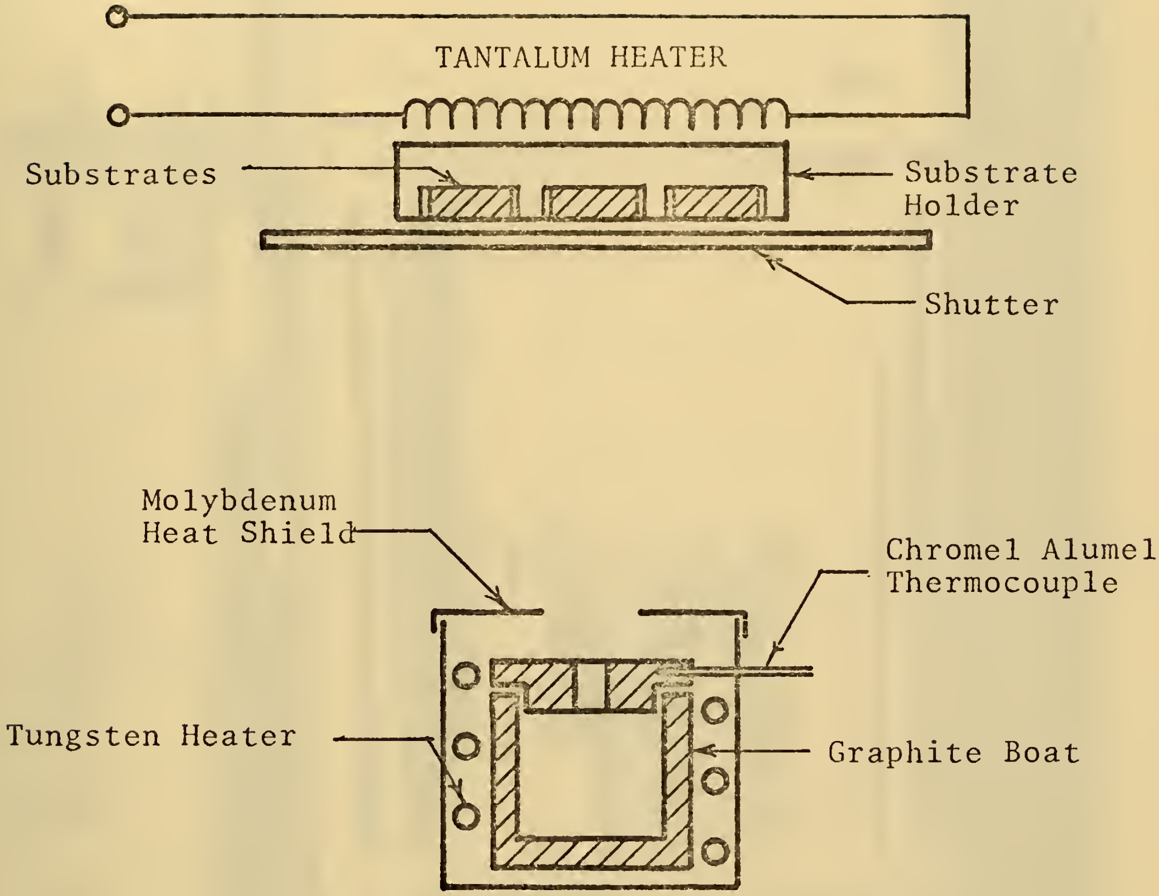

Figure 5

Deposition Unit (Diagram)

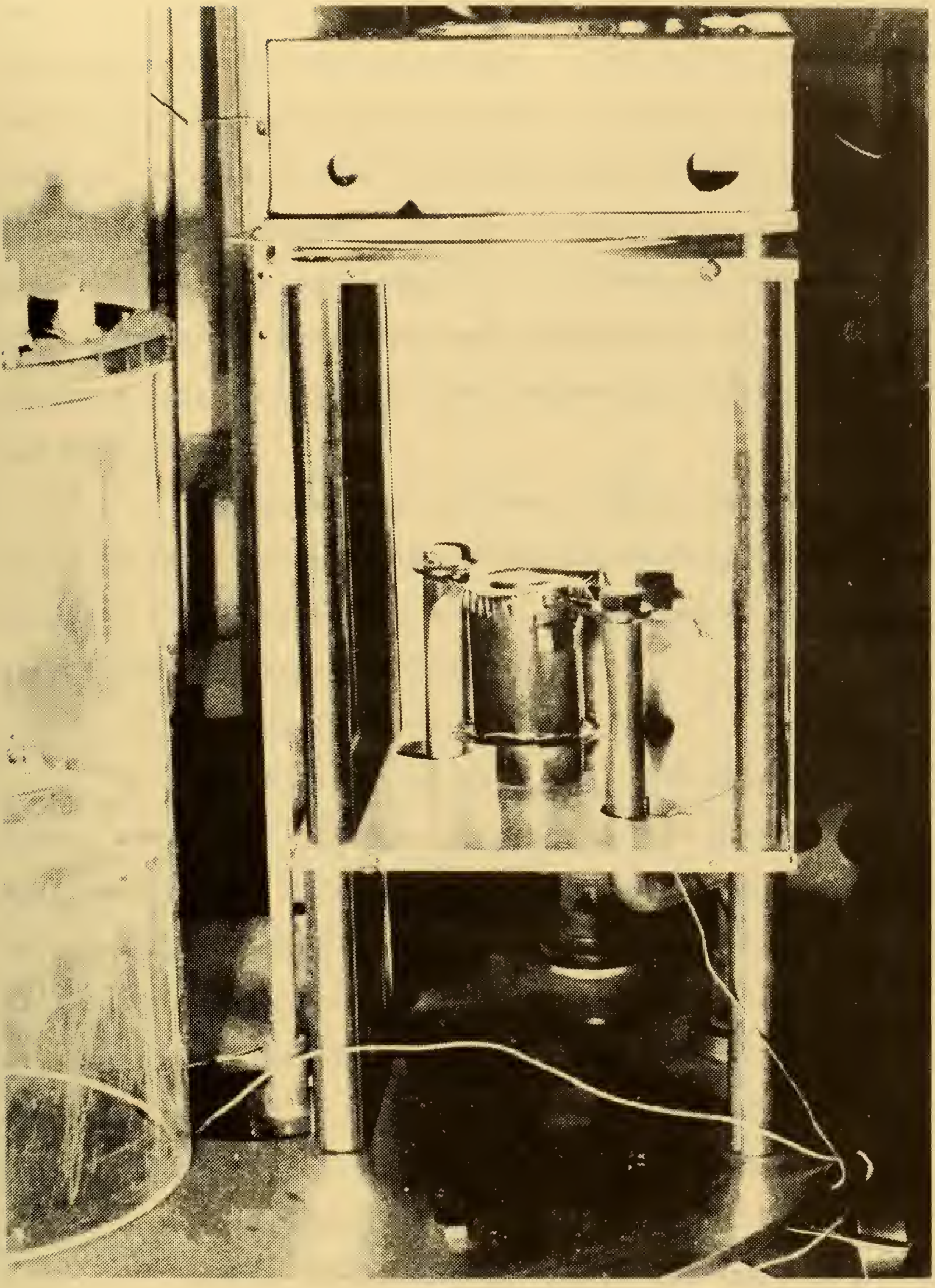

Figure 6
Deposition Unit

one of the samples. The thermocouple was used to control the temperature of the substrates. The holder assembly was heated by a tantalum ribbon heater. The boat was cut from graphite on a lathe and was approximately one inch in diameter and one inch in height. It was placed inside a tungsten basket heater and surrounded by a molybdenum heat shield. A chromel alumel thermocouple was inserted in the lid of the graphite boat so that the boat temperature could be monitored and controlled.

The substrate and the graphite boat temperatures were controlled by two time proportioning controllers. The diagram of the deposition system, including related controlling units, is shown in Figure 7.

b. Deposition Procedures

Small chunks of $Pb_{0.80}Sn_{0.20}Te$ were used as source materials. They were loaded in the graphite boat which had a hole of 1/16 inch in the top. Substrates were obtained by cleaving single crystal BaF_2 and CaF_2 substrate in a laminar flow hood to prevent foreign matter from condensing on the freshly cleaved surface. The substrates were then mounted in the stainless steel substrate holder and a chromel alumel thermocouple mounted to the face of one of the substrates.

After the source materials and the substrates were loaded in the vacuum system, the system was pumped down to the mid-10^{-6} torr range in approximately one hour.

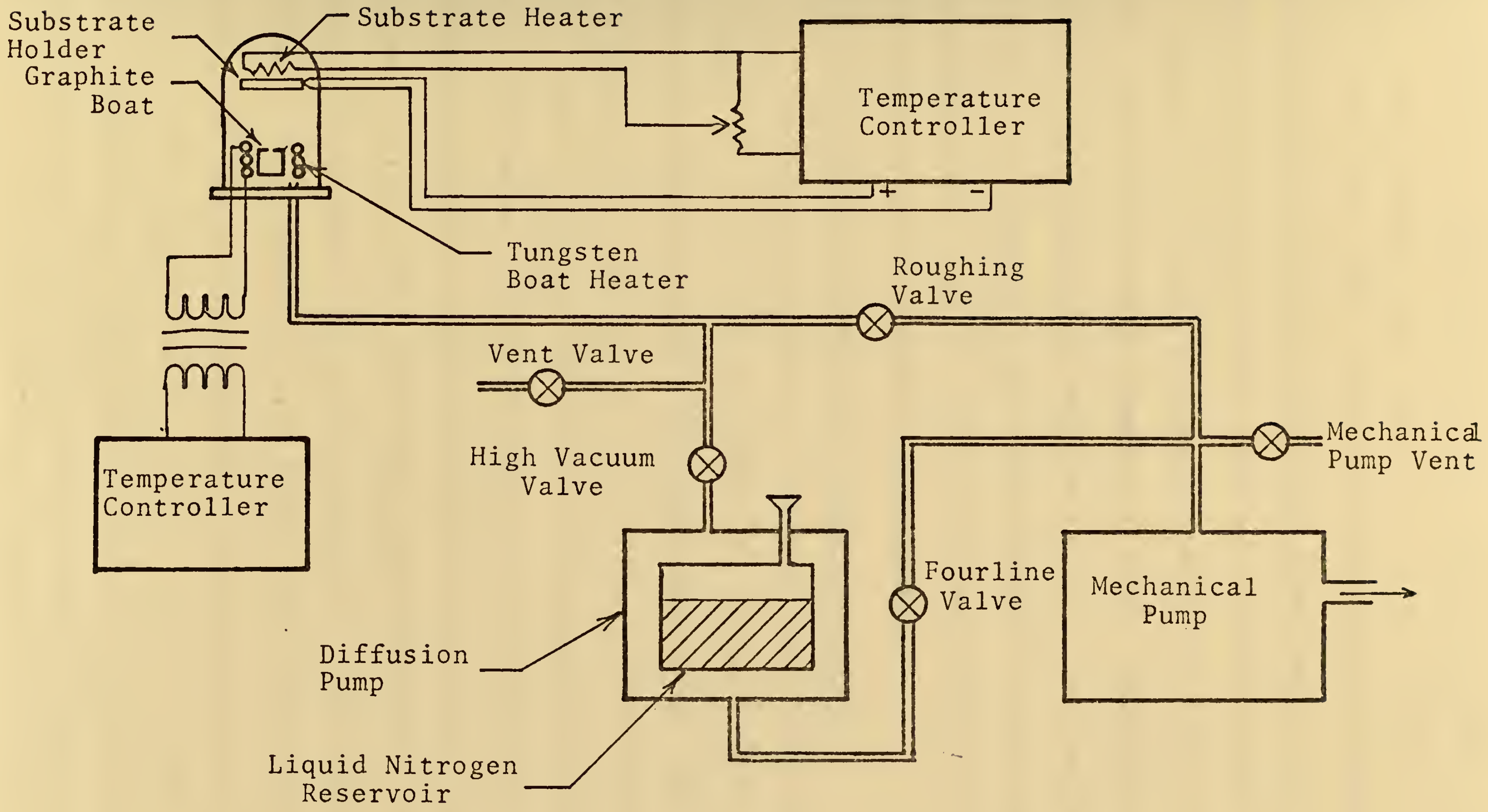

Figure 7

Deposition System Block Diagram

The substrate temperature was then raised to values around 300°C. The graphite boat temperature was raised to a value between 700°C and 800°C. Shortly after the boat temperature had stabilized, the shutter was opened and deposition began. Deposition took place at the rate of 2-3 microns per hour. The shutter was allowed to remain open for a time estimated to give the desired film thickness. After deposition, the substrate temperature was reduced to 200°C and maintained for two hours. The samples were then allowed to cool down to room temperature typically over a period of four hours before being removed from the deposition chamber.

3. Isothermal Annealing of Deposited Films

Isothermal annealing techniques have previously been developed for bulk Pb-Sn chalcogenide crystals [Ref. 12] and successfully employed for $Pb_{1-x}Sn_xTe$ thin films [Ref. 40]. The principle will be explained briefly in the following.

The $Pb_{1-x}Sn_xTe$ alloys are stoichiometric semiconductors. The number of free carriers is believed to be directly proportional to the deviation from stoichiometry. For $Pb_{1-x}Sn_xTe$ alloys, the thin films prepared by one boat evaporation methods, using stoichiometric starting source materials, were found to be p-type. The p-type majority carriers in the as-deposited thin films were believed to be due to Pb Sn deficiencies and/or excess Te ions. This was an extension of the well known experimental results that excess lead and excess chalcogenide defects behave as donors

and acceptors, respectively, in the lead salts such as PbTe, PbSe and PbS.

It is felt that the carrier concentrations resulting from nonstoichiometrics in these films are much larger than the carrier concentrations resulting from the impurities in the materials. The carrier type and concentration is primarily determined by the deviation from stoichiometry. These nonstoichiometrics can be altered by the isothermal annealing technique which was first developed by Brebrick and Allgaier for PbTe [Ref. 41]. They can also be altered by irradiation with high energy particles which is the subject of this thesis research.

The phase diagram of a typical $Pb_{1-x}Sn_xTe$ alloy is shown in Figure 8. The effect of the isothermal annealing can be explained by this phase diagram which involves the equilibrium under isothermal condition of an alloy of known composition outside the solidus field with a crystal of a preselected initial defect concentration. In practice the p-type as-deposited thin film was isothermally annealed with a PbSn rich alloy of the same composition very near the stoichiometric temperature, T_o, where the metal saturated solidus curve intersects with the ideally stoichiometric line. Theoretically, under this condition, the crystal with arbitrary initial concentrations would shift toward the stoichiometric line. The stoichiometric temperature, T_o, changes with the composition of the alloys involved, and

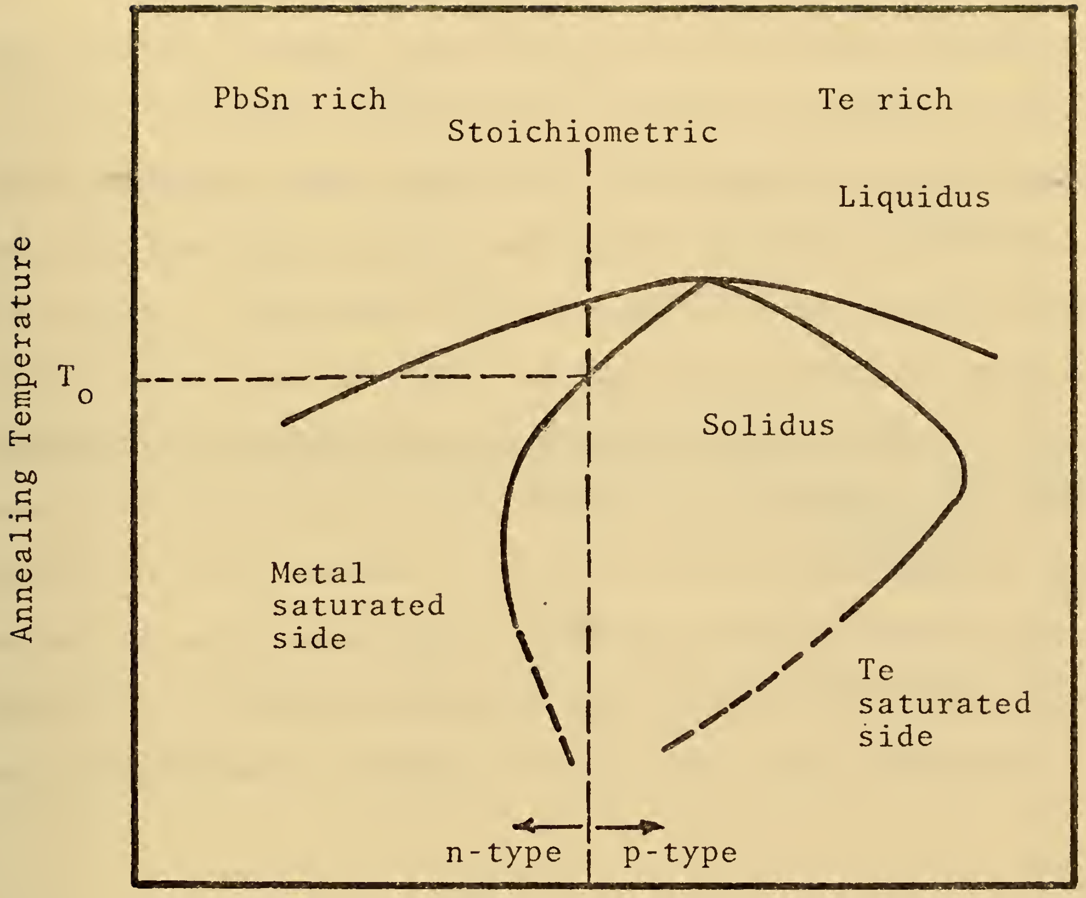

Figure 8

Phase Diagram of a Typical $Pb_{1-x}Sn_xTe$ Alloy

was determined experimentally for $Pb_{0.80}Sn_{0.20}Te$. Both p-type and n-type samples were obtained for these thin film alloys.

Isothermal annealing was performed as follows. Small chunks of metal rich materials of the same composition as the film being annealed were sealed in specially shaped quartz ampoules (see Figure 9). The ampoule was evacuated and refilled with 100-200 mmHg of dry Helium gas before it was sealed. The purpose was to supply certain vapor pressure in the closed tube so that the thin film crystals would not sublimate excessively during the annealing process. The metal rich materials were prepared by the method described earlier in this section. Usually two or three samples were sealed in each ampoule and separated from the metal rich material. A complete equilibrium condition for bulk crystals was established by Calawa, et al. [Ref. 12] as follows:

$$\frac{Dt}{d^2} > 1 \qquad (2\text{-}1)$$

where: D is the diffusion coefficient
d is the thickness of the sample and
t is the annealing time.

Since the diffusion coefficient for $Pb_{0.80}Sn_{0.20}Te$ has not yet been determined, equilibrium time for $Pb_{0.80}Sn_{0.20}Te$ thin film could not be established. The annealing time was therefore established by trial and error from the general behavior of the electrical properties of the annealed samples.

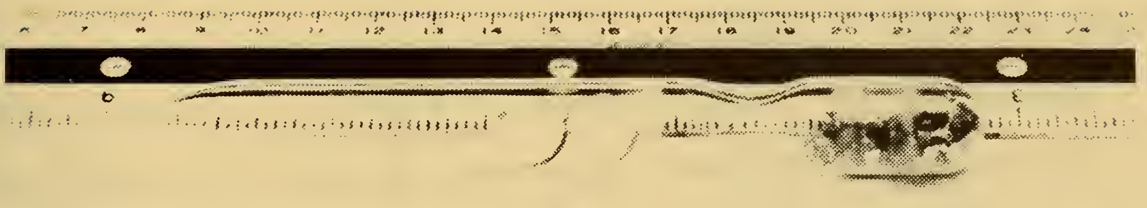

Figure 9
Ampoule Ready for Isothermal Annealing

The sealed ampoules were placed in a regulated Marshall furnace (see Figure 10) at selected temperatures and time periods typically around 540°C and three hours. The schematic diagram of the annealing furnace is shown in Figure 11. Temperatures were monitored by a chromel alumel thermocouple and a Leeds and Northrup potentiometer.

Some annealing was done in a furnace equipped with a Dynatherm isothermal furnace liner filled with sodium metal to give a longer region of uniform temperature. Without the liner a section within the furnace approximately three inches displayed a uniform temperature. With the liner this region was extended to twelve inches. It was within the region of constant temperature that the annealing was carried out. The temperature was maintained to within one degree of the desired annealing temperature by a Marshall temperature controller and monitored using a Leeds and Northrup potentiometer. At the end of the annealing period the ampoule was withdrawn from the oven in stages over a period of five minutes to avoid thermal shock and the subsequent cracking of the sample substrates. After removal the sample was allowed to cool to room temperature by ambient cooling.

4. Preparation of Electrical Contacts

It was this stage of sample preparation that resulted in the greatest reduction of sample yield. The sample used (see Figure 12) was made by depositing pure gold on the

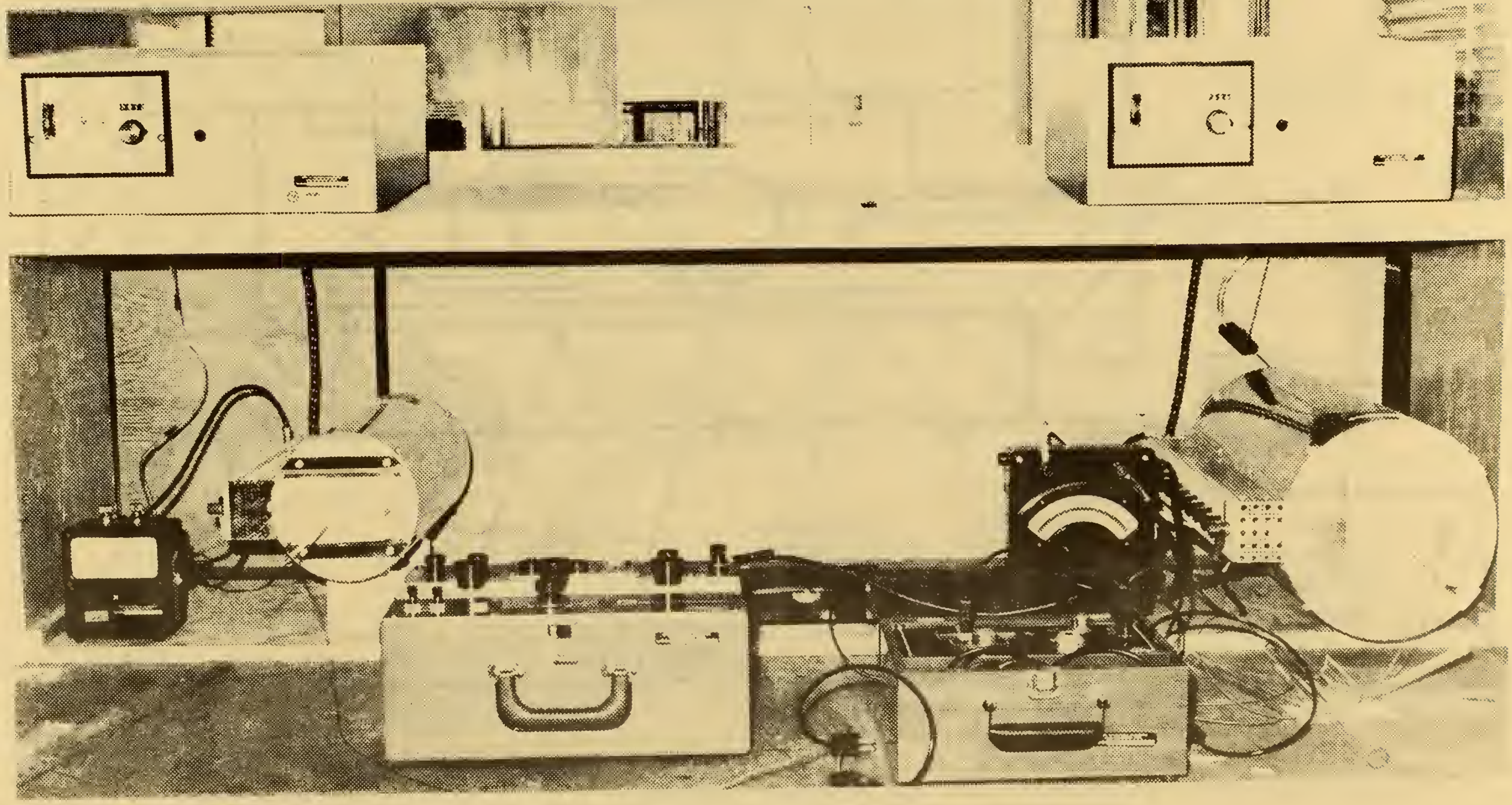

Figure 10
Annealing Furnaces

[illegible]

[illegible]

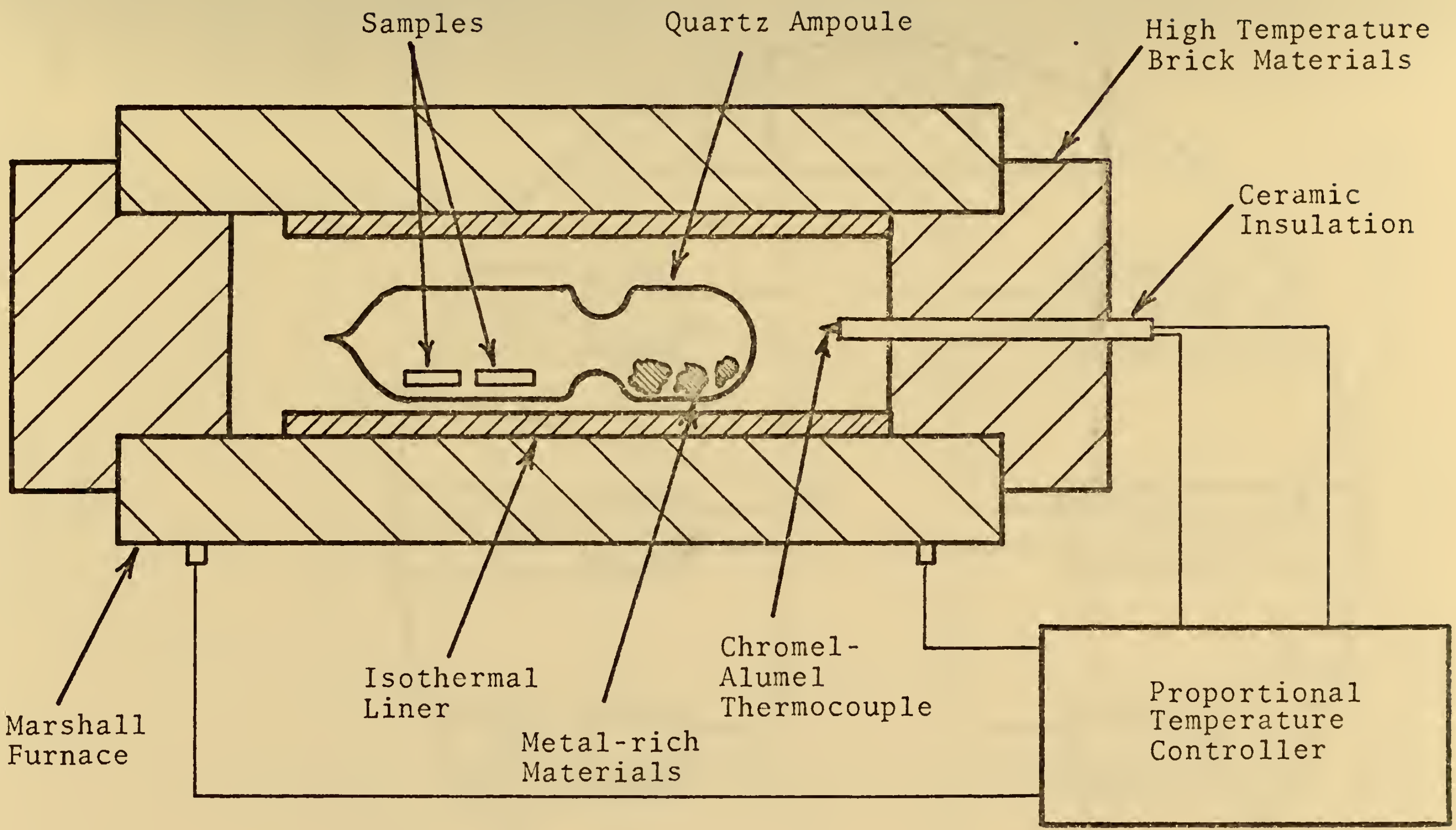

Figure 11

The Annealing Apparatus

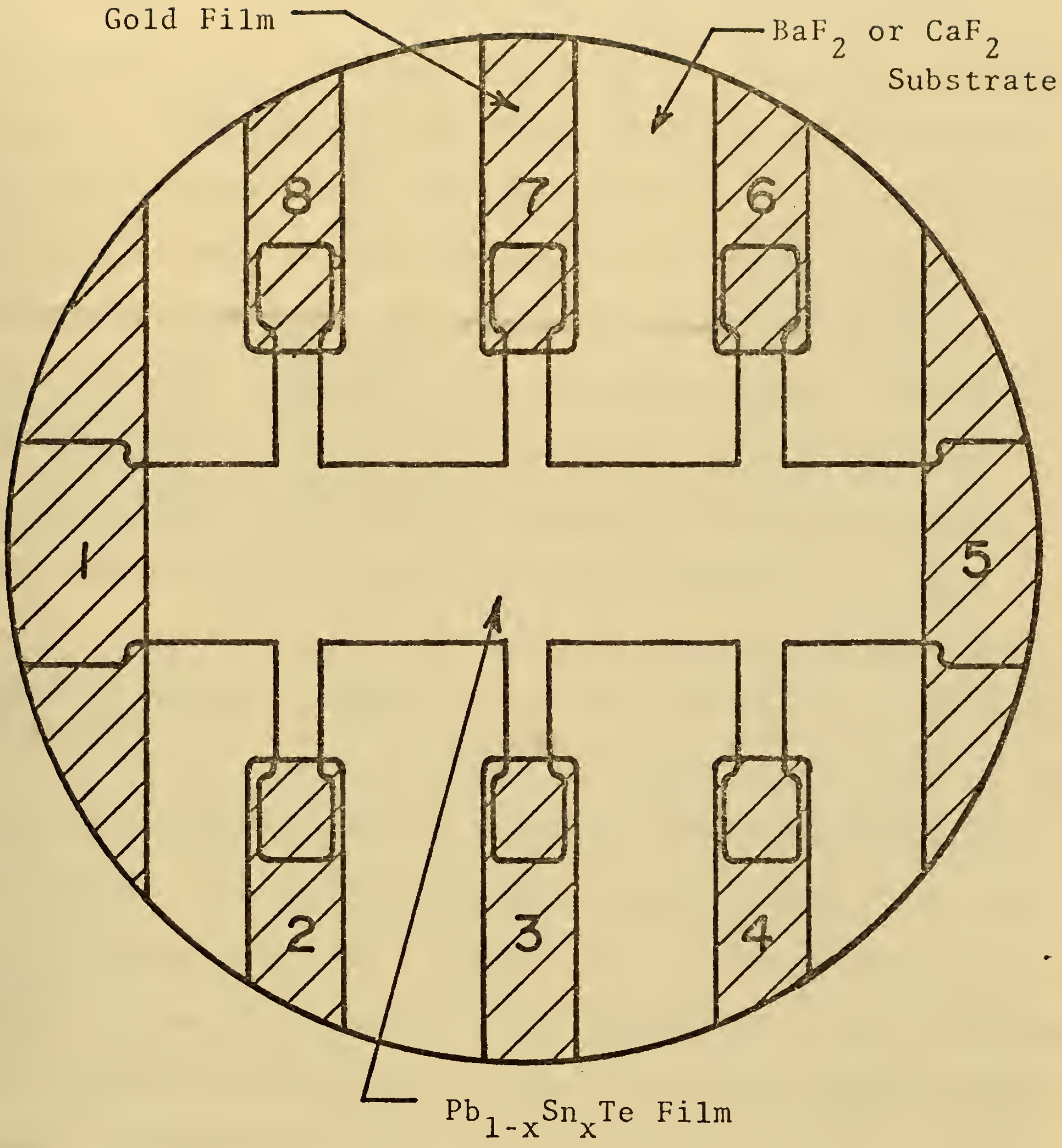

Figure 12

Hall Sample

sample through a mask to limit the sample area of 0.2 cm^2 and to make it possible to attach electrical contacts (see Figure 13). Contacts 1 and 5 were the current contacts. Contacts 2, 3, 4, 6, 7 and 8 were used for conductivity and Hall measurements. Having several sets of measurement contacts allowed a check on sample uniformity as well as offering a back-up in the event of contact failure.

It was found that the adhesion of some samples to the substrate was not strong enough to support wire in excess of five mils diameter during the transition from room temperature to liquid nitrogen temperature. As a result, cooper or gold wire of two to three mils diameter proved to be more reliable although somewhat more difficult to work with. Several methods of attaching the wire to the gold contact regions were attempted with varying degrees of success. The most reliable procedure proved to be the use of silver epoxy even though these contacts sometimes lifted at low temperatures. The small wires from the sample were soldered to terminals on the dewar cold finger (see Figures 14 and 15).

B. EVALUATION OF DEPOSITED FILMS

1. Determination of Film Thickness

After the sample had been annealed and gold pads deposited, film thickness measurements were made using a Perkin Elmer Infracord Spectrophotometer (see Figure 16). Transmittance measurements were taken (see Figure 17)

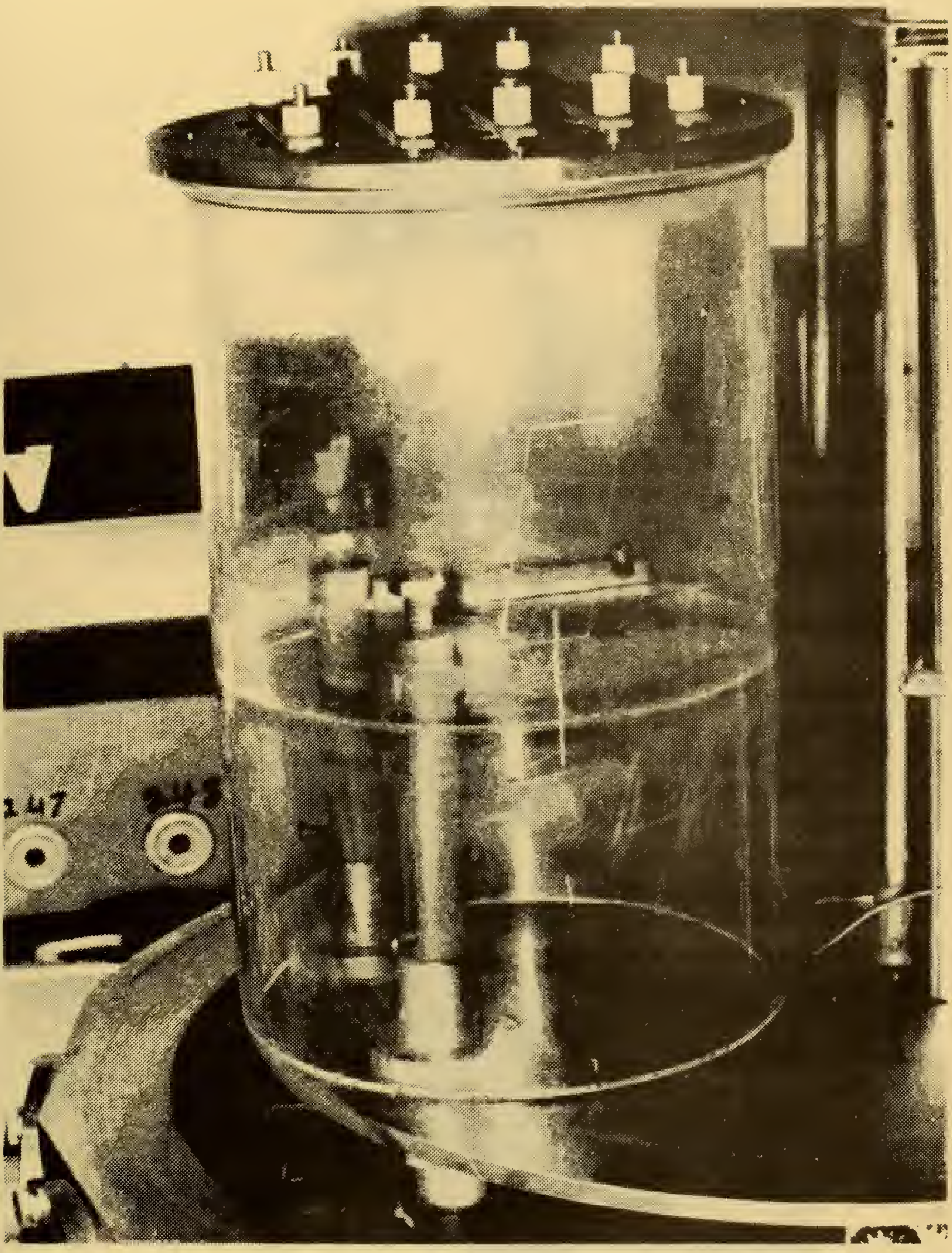

Figure 13

Gold Deposition Chamber

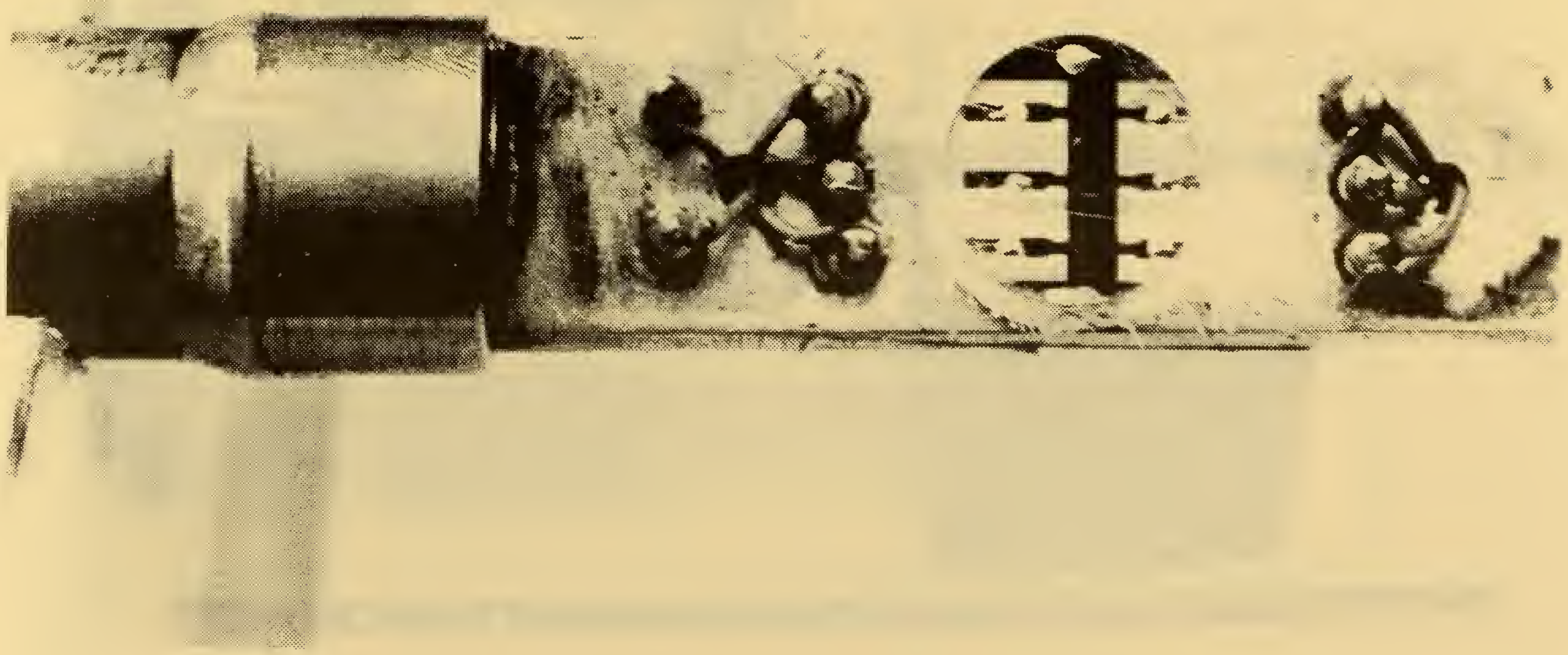

Figure 14
Sample Mounted on Dewar

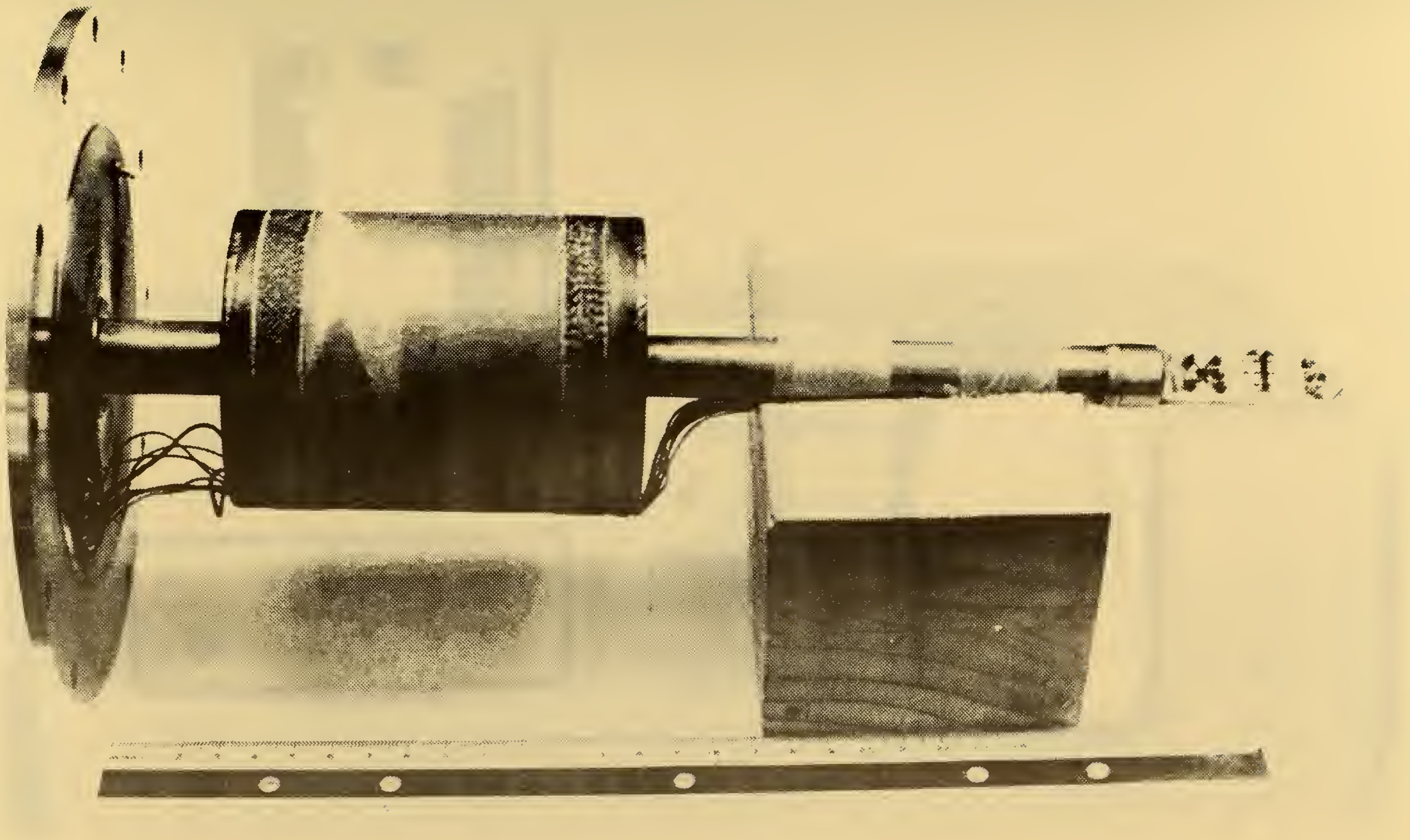

Figure 15
Inner Dewar

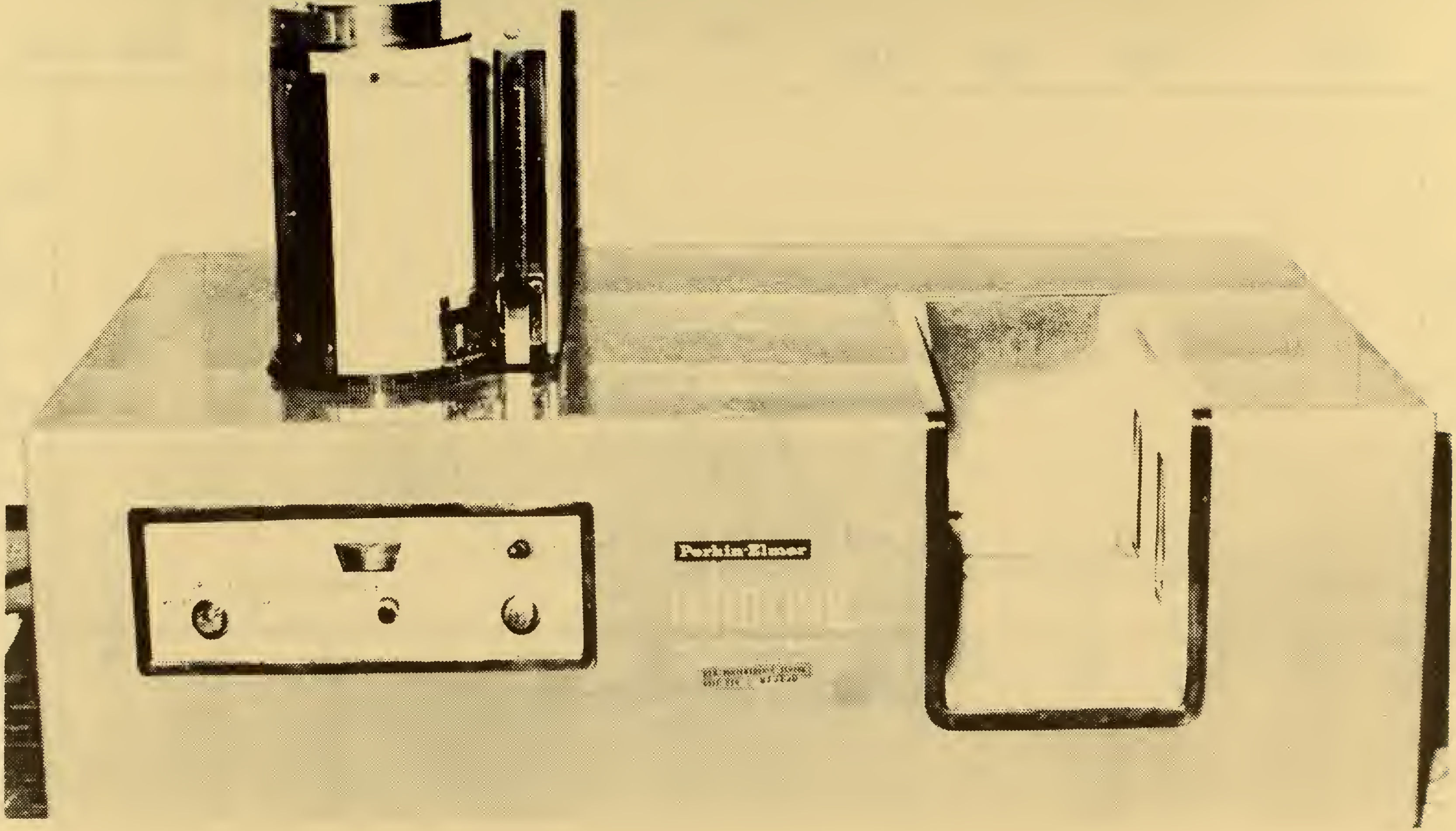

Figure 16
Spectrophotometer

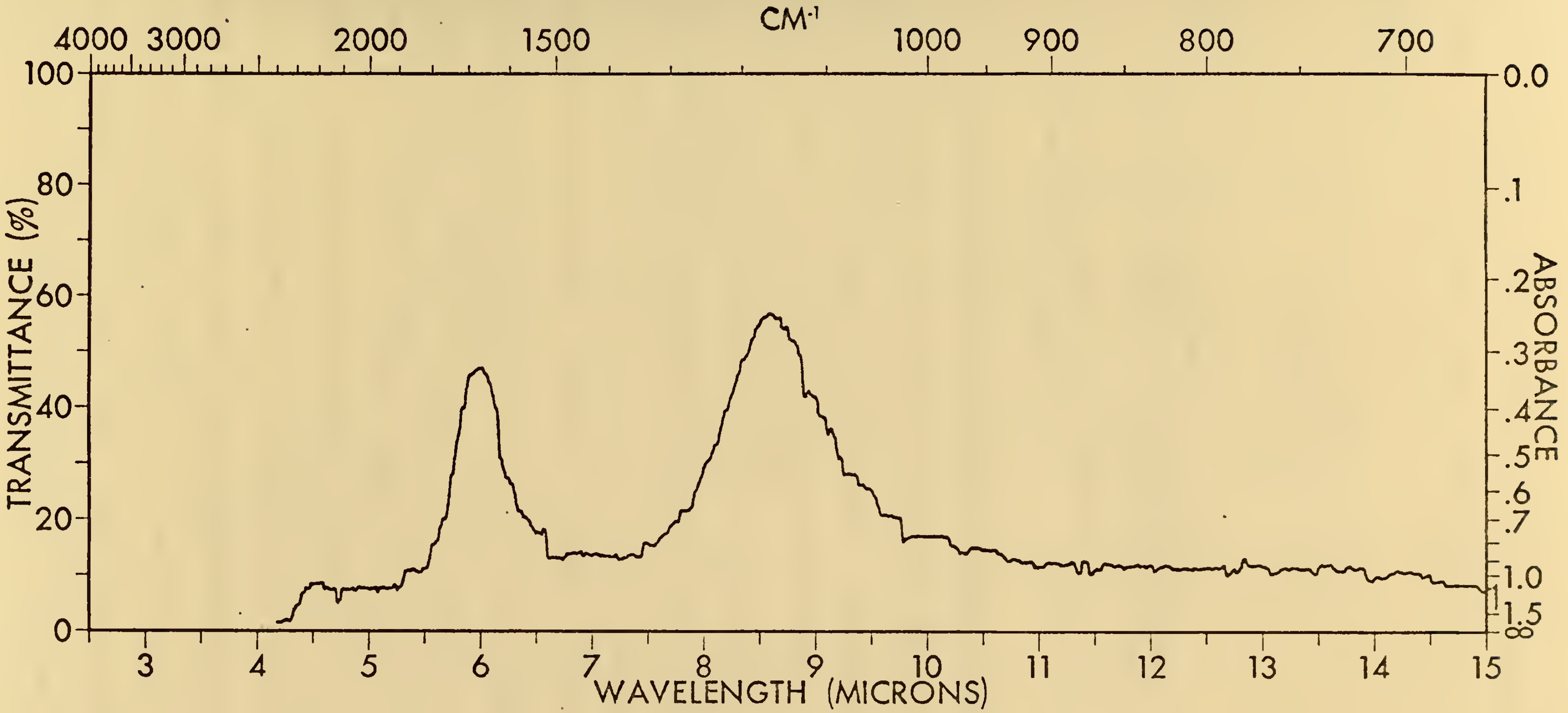

Figure 17

Transmittance measuremant data
for determining thickness

although in some cases reflectance measurements had to be used. The thickness was determined from the following equation:

$$d = \frac{m \times 10^4}{2n(\nu_1 - \nu_2)} \qquad (2\text{-}2)$$

where: d is the thickness in microns
m is the number of waves between ν_1 and ν_2
n is the index of refraction (5.9)^1
ν_1 and ν_2 are the frequencies (cm^{-1}) of the interference peaks.

2. Determination of Carrier Concentration and Mobility

To study the effects of proton bombardment, a method of evaluating the electrical properties of the material before and after bombardment must be available. In this research the Hall effect and conductivity measurements were used to determine the carrier concentration, carrier type and mobility. The block diagram of the electrical measurement system is shown in Figure 18. A photograph of the electrical measurement apparatus is shown in Figure 19. The Hall sample was mounted on the cold finger of a liquid nitrogen dewar with silicon heat sink compound to ensure good thermal conductivity. A blank substrate was mounted on the opposite side of the cold finger and a copper-constantan thermocouple placed on the blank substrate so that the temperature of the Hall sample could be recorded. The electrical contacts were connected as previously described. The inner dewar was

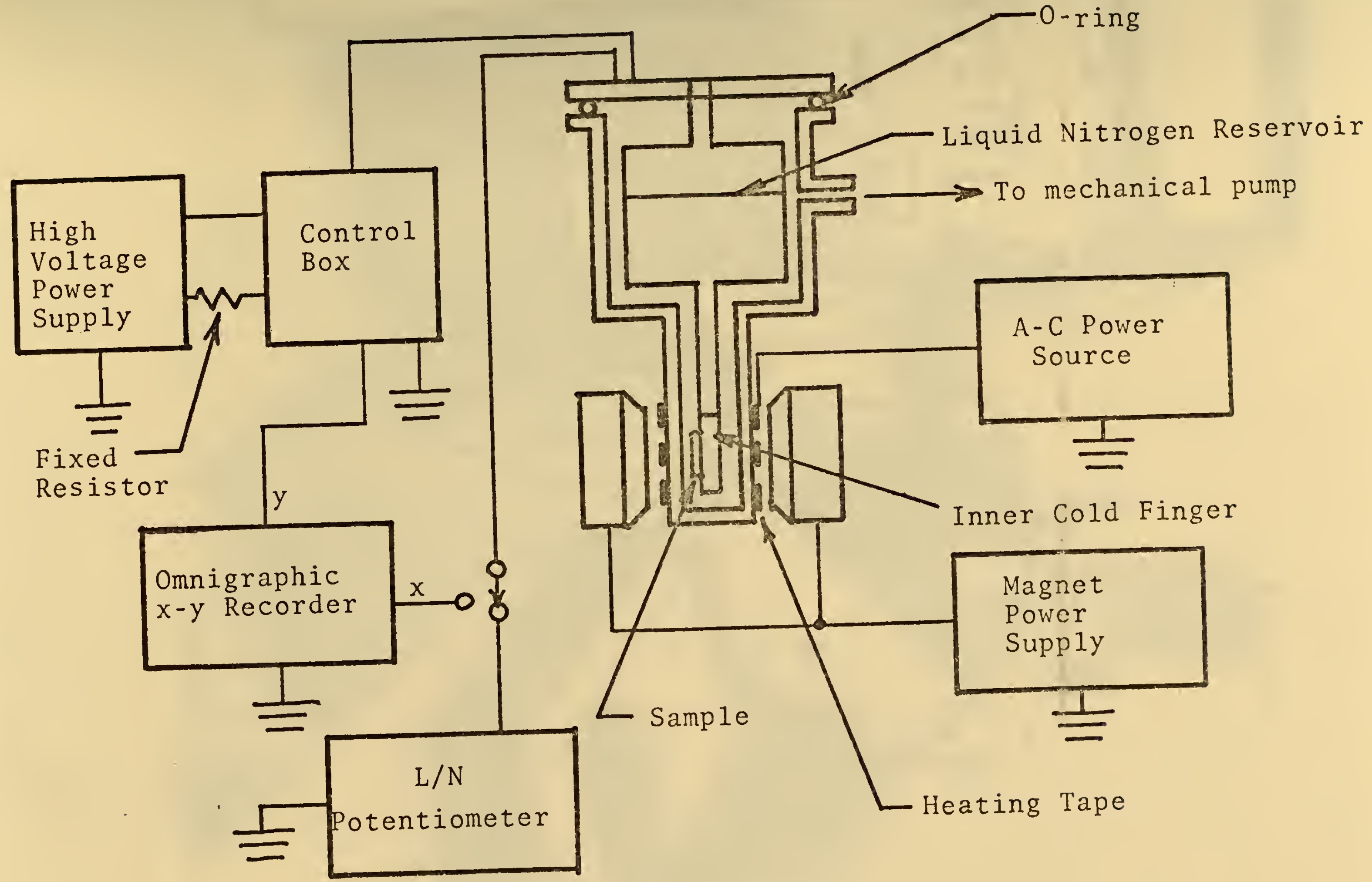

Figure 18

Block Diagram of the Electrical Measurement System

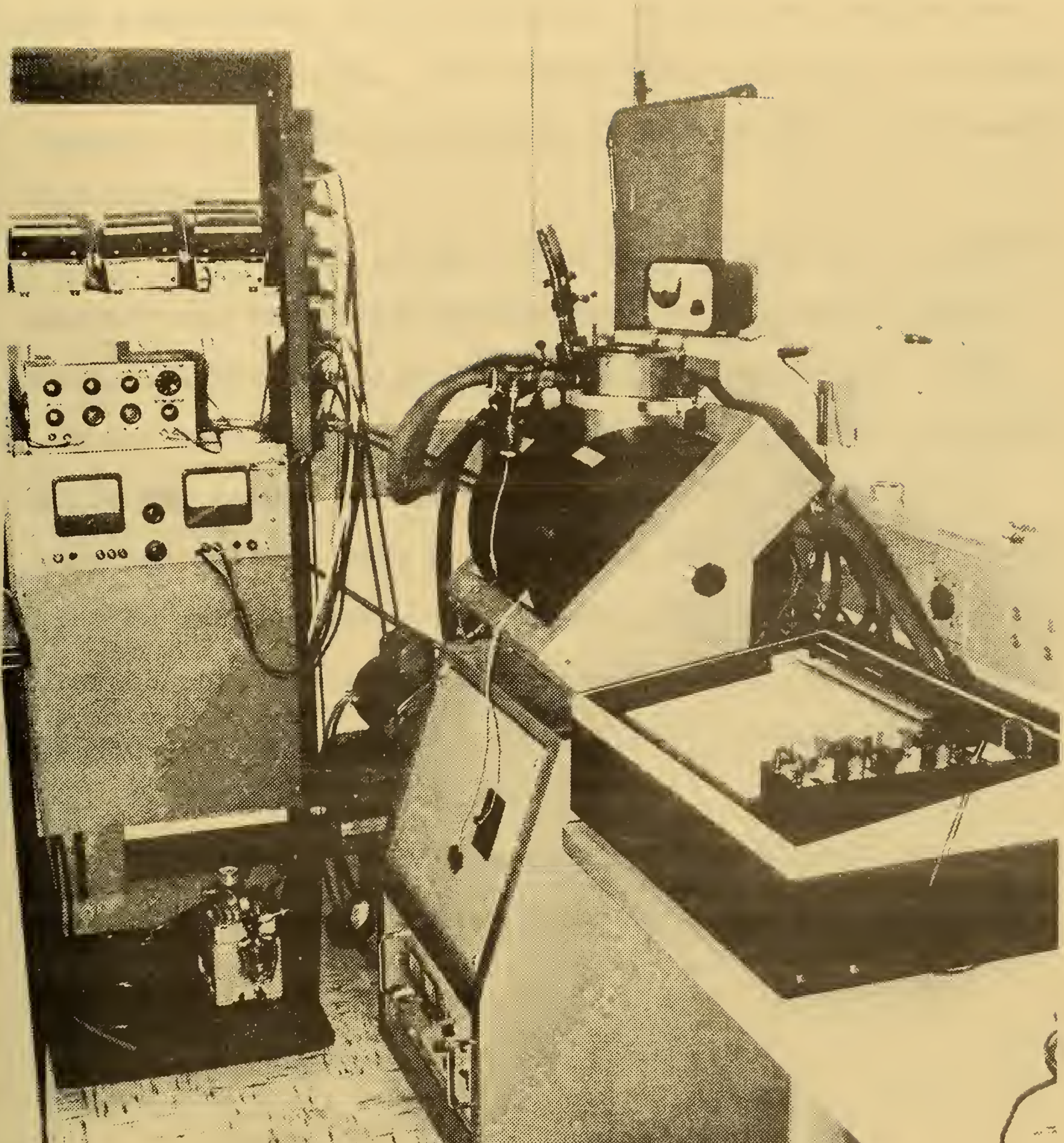

Figure 19
Electrical Measurement Apparatus

placed in the vacuum chamber and sealed. The system was then pumped down to approximately 20 microns before measurements were begun. The vacuum was necessary to prevent condensation of moisture vapor on the sample as the sample was cooled.

A constant current of 1 ma. was passed through the sample (see Figure 18) from a high voltage power supply through a fixed resistor during the measurements. The conductivity voltage was recorded as the sample was cooled. While the sample slowly warmed, the Hall voltages were recorded while a 5000 gauss magnetic field was alternately applied and removed. By smoothing the curves, a continuous plot of potentials with and without the field could be obtained (see Figure 20). The difference between the two was the Hall voltage, V_H.

The Hall coefficient, R_H(cm^3/coul) and the conductivity, σ, were calculated from the following relations:

$$R_H = \frac{V_H \text{ x } d}{B \text{ x } I} \qquad (\text{cm}^3/\text{coul}) \qquad (2\text{-}3)$$

$$\sigma = \frac{26900 \text{ x } I}{V_c \text{ s } d} \qquad (1/\text{ohm-cm}) \qquad (2\text{-}4)$$

where V_H and V_c are the Hall and conductivity voltages respectively in millivolts. The sample current, I, is in milliamperes. The magnetic induction, B, is in Webers/m^2

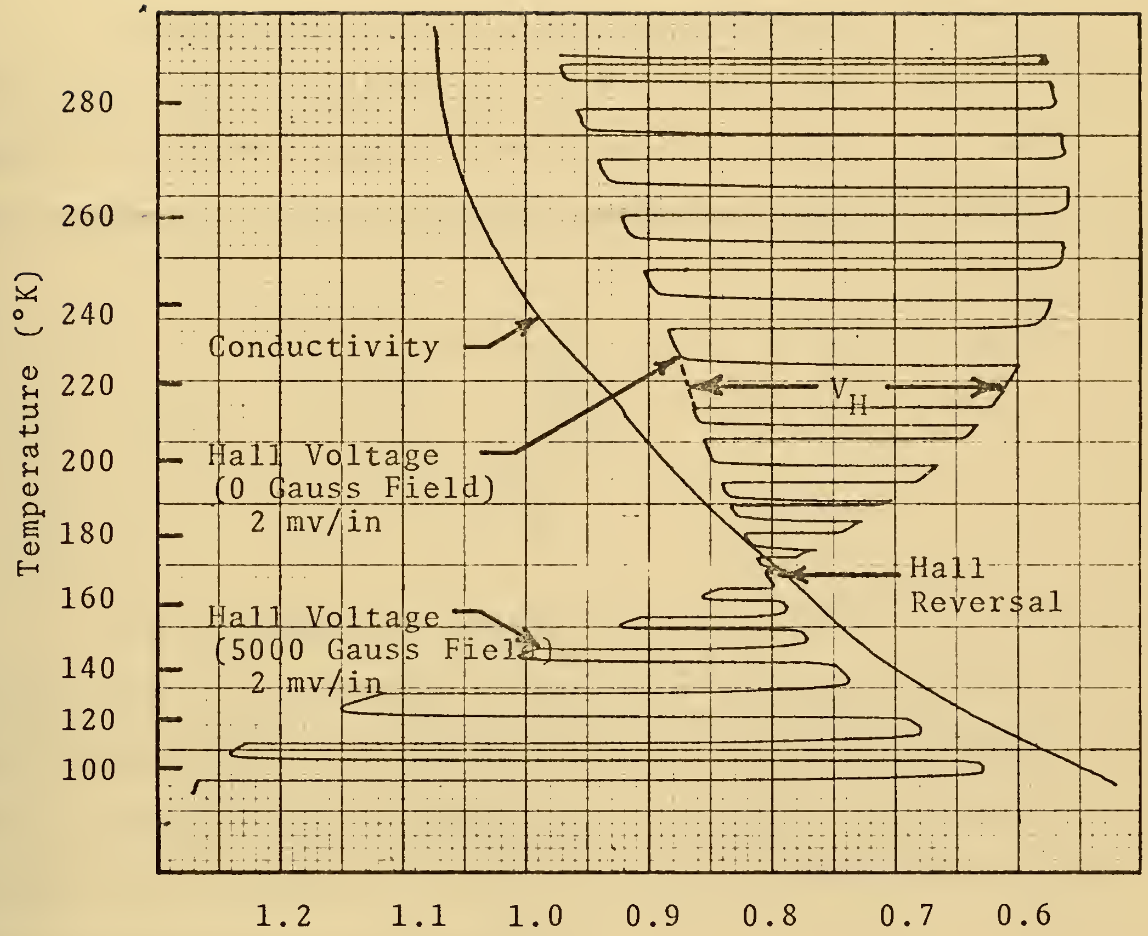

ST 20 OBX 9-4 Sample #47 after proton bombardment of 2 x 10^{14} protons/cm^2

Figure 20
Electrical Measurement Output

and d is the thickness of the sample in microns. The numerical factor, 26900, is from the physical dimensions of the Hall sample.

The majority carrier concentrations and the Hall mobilities are calculated by the following equations if the sample is either strongly n or p type, in which case only the properties of the majority carrier need be calculated:

$$n \text{ (or } p) = \frac{1}{q\,R_H} \qquad (2\text{-}5)$$

$$\mu_H = R_H\sigma$$

If the sample is nearly intrinsic (weak p or n type), a Hall reversal, or shift in majority carrier, may occur at some temperature as shown in Figure 21 which was reduced from the data shown in Figure 20. In such a case the following equations must be solved in order to obtain the carrier concentration and mobility:

$$R_H = \frac{H_h p - H_e n b^2}{q(p+nb)^2} \qquad \text{(for ellipsoidal energy surface [Ref. 42])} \qquad (2\text{-}6)$$

$$\sigma = nq\mu_e + pq\mu_h \qquad (2\text{-}7)$$

$$b = \frac{\mu_e}{\mu_h} \qquad (2\text{-}8)$$

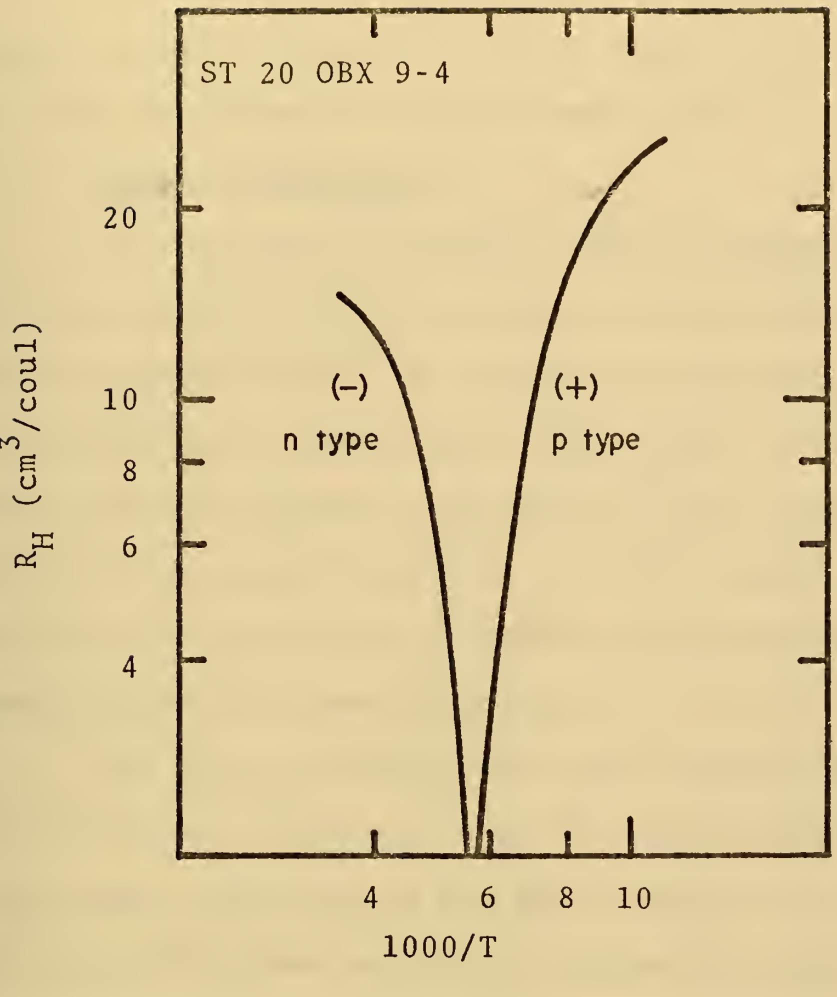

Figure 21

Plot of Hall Factor

where μ_e and μ_h are the mobilities for electrons and holes, respectively. H_e and H_h are Hall factors for electrons and holes, respectively.

In the case of nearly intrinsic samples, the computer program listed at the end of this study was used to determine carrier concentrations and mobilities.

3. Proton Bombardment

As previously explained, the as-deposited thin films were p-type and had carrier concentrations in the order of low $10^{18}/cm^3$. By the isothermal annealing techniques described in Section II-A-3, p-type samples with carrier concentrations in the mid $10^{17}/cm^3$ were prepared. After the electrical properties of these samples were measured and recorded, each sample was bombarded at room temperature with a beam of protons.

The proton irradiations were carried out using Naval Ordnance Laboratory's 2.5 MV Van de Graaf accelerator. As the normal beam energy was much higher than desired for this study, the beam energy was reduced by passing it through a 1.0 mil aluminum foil. A calibration curve was obtained of the exit particle energy vs. the incident beam energy by measuring the proton energy after it had passed through the foil attenuator. These measurements were made at an exit angle of about five degrees to the incident beam using a solid state surface barrier silicon particle detector. The samples bombarded were irradiated at a beam energy of 250 KeV (incident beam on aluminum absorber of 1.65 MeV).

For the irradiation of the samples the fluence (number of protons/cm^2) was obtained by measuring the total charge from the incident beam collected on the target. The fluence is given by:

$$F = \frac{\text{total charge collected in Coulombs}}{\text{beam area} \times 1.6 \times 10^{-19}} \qquad (2\text{-}9)$$

The beam area was obtained by directly measuring the area being irradiated on a quartz viewer which was placed temporarily where the thin film samples were to be placed. The quartz viewer flouresced (blue) where it was being struck by the beam. During the sample irradiation, care was taken to insure that the beam current was properly measured. Figure 22 shows the geometry that was used. The purpose of the -1000 V aperture is to eliminate the possibility of secondary electrons being collected by or lost from the target thereby giving a false indication of the total charge collected. The current integrator was an Elcor Model A309B Current Indicator and Integrator. It automatically signaled when a preset charge was accumulated; thus it could be preset for the total fluence desired by equation (2-9) and interrupt the beam from the target sample.

4. Isochronal Annealing

Like all other radiation effects, proton bombardment is believed to create vacancies and interstitial atoms in the

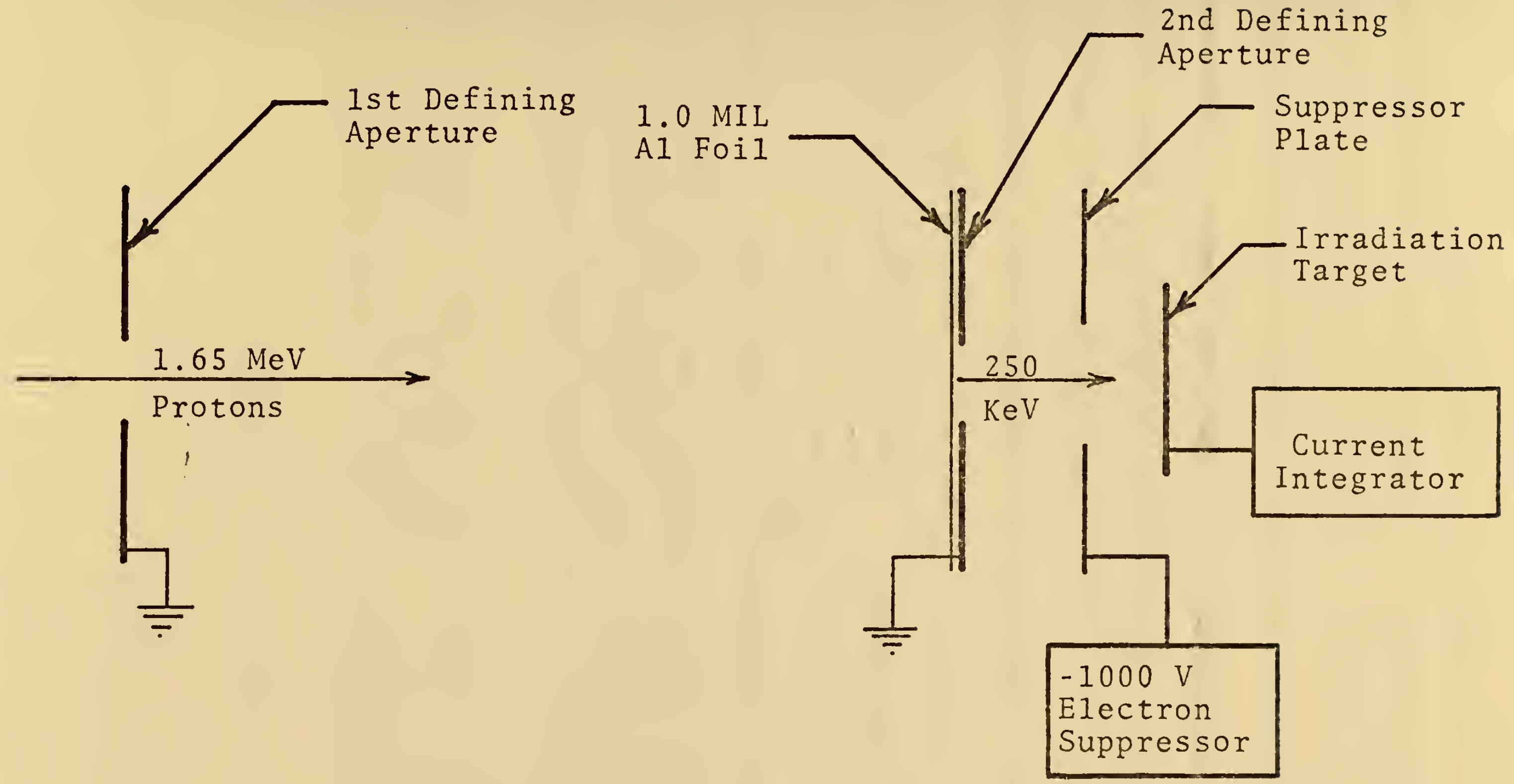

Figure 22

Proton Irradiation System

semiconductor material. By the principle of thermodynamics, raising the temperature of the material raises the free energy. It is expected that the effect of proton bombardment can be altered by heat treatment. For our $Pb_{0.80}Sn_{0.20}Te$ thin films, isochronal or pulsed annealing was performed to investigate the recovery of the proton bombardment effect.

Isochronal annealing was carried out with the sample mounted on the dewar cold finger (Figure 18). The vacuum chamber was back-filled with dry helium gas to provide thermal conduction while preventing sample sublimation at elevated temperatures. The sample was heated by the heating tape wrapped outside the dewar. Successively higher temperatures in twenty degree increments for a period of ten minutes each were used. The electrical properties down to liquid nitrogen temperatures were measured after each annealing period. Isochronal annealing was carried out to 180°C or until the sample became unusable due to contact failure.

III. RESULTS AND DISCUSSION

During the performance of this research, $Pb_{0.76}Sn_{0.24}Te$ samples were used in addition to $Pb_{0.80}Sn_{0.20}Te$ samples. The results from these samples were compared to results from previous research to ensure that the experimental methods were consistent. In all cases the results were in agreement with previously published results. Having results from the 24% sample available also allowed some comparisons to be made based on alloy compositions.

A. ISOTHERMAL ANNEALING

The results of isothermal annealing are shown in Table I and in Figure 23. There are several factors that may have caused the apparent discrepancies between the isothermal annealing temperatures and the resulting carrier concentrations. The first factor is the alloy composition of the materials involved. Slight errors in the alloy composition can have a significant effect on the stoichiometric temperature, T_o. For example, the stoichiometric temperature, T_o, for $Pb_{0.76}Sn_{0.24}Te$ is approximately 518°C so, by interpolation, an error of only 0.125% in alloy composition leads to a change in T_o of one degree centigrade. The second factor is the variation involved in the annealing process. The temperature controllers used were only accurate to within ±1°C and showed some drift from day to day.

TABLE I

ISOTHERMAL ANNEALING OF $Pb_{0.80}Sn_{0.20}Te$ THIN FILMS

Sample Number	Deposition Number	Thickness (microns)	Annealing Temperature (°C)	Annealing Time (min)	Carrier Concentration (cm^{-3} @ 90°K)	Mobility (cm^2/v-sec @ 90°K)
5	ST 20 OBX 1-2	0.99	540	180	5.3×10^{17} (p)*	790
6	ST 20 OBX 1-3	0.91	540	180	5.4×10^{17} (p)	280
8	ST 20 OBX 2-1	1.13	540	180	3.6×10^{17} (p)	780
10	ST 20 OBX 2-2	1.07	540	180	3.3×10^{17} (p)	1500
11	ST 20 OBX 2-3	1.08	540	180	3.0×10^{17} (p)	1000
12	ST 20 OBX 2-4	1.15	541	178	2.8×10^{17} (p)	360
13	ST 20 OBX 2-5	1.21	541	178	2.5×10^{17} (p)	520
15	ST 20 OBX 3-1	1.68	541	160	2.5×10^{17} (p)	1160
24	ST 20 OBX 5-5	1.69	538.5	145	6.6×10^{17} (n)	560
46	ST 20 OBX 9-3	1.01	540	180	2.2×10^{17} (p)	380
47	ST 20 OBX 9-4	0.94	540	180	2.5×10^{17} (p)	1570
49	ST 20 OBX 10-1	1.80	540	180	4.4×10^{17} (p)	130
51	ST 20 OBX 10-4	1.70	540	180	3.1×10^{17} (p)	170
53	ST 20 OBX 11-1	0.95	539	180	9.7×10^{17} (p)	300
62	ST 20 K 3-3	2.42	541.5	180	3.9×10^{17} (p)	13000
63	ST 20 K 3-5	1.76	541.5	180	4.2×10^{17} (p)	400

* (p) for p-type samples, (n) for n-type samples

TABLE I (continued)

Sample Number	Deposition Number	Thickness (microns)	Annealing Temperature (°C)	Annealing Time (min)	Carrier Concentration (cm^{-3} @ 90°K)	Mobility (cm^2/v-sec @ 90°K)
68	ST 20 K 5-2	1.30	539	180	1.3×10^{18} (p)	30
71	ST 20 K 6-4	1.46	539.25	179	1.7×10^{17} (n)	300
72	ST 20 K 6-5	1.46	540.5	180	5.9×10^{17} (p)	3300
73	ST 20 K 7-1	1.73	539.75	180	1.0×10^{17} (n)	1500
77	ST 20 K 7-5	1.57	539	180	4.1×10^{17} (p)	160
78	ST 20 K 9-1	1.66	540.5	180	9.9×10^{17} (n)	4100
79	ST 20 K 9-2	1.71	539.75	180	1.4×10^{17} (n)	1700
80	ST 20 K 9-3	1.69	539	180	6.8×10^{17} (n)	10000
82	ST 20 K 9-5	1.51	541.5	180	3.2×10^{17} (p)	460
84	ST 20 K 8-5	1.57	540.5	180	2.1×10^{17} (n)	1100

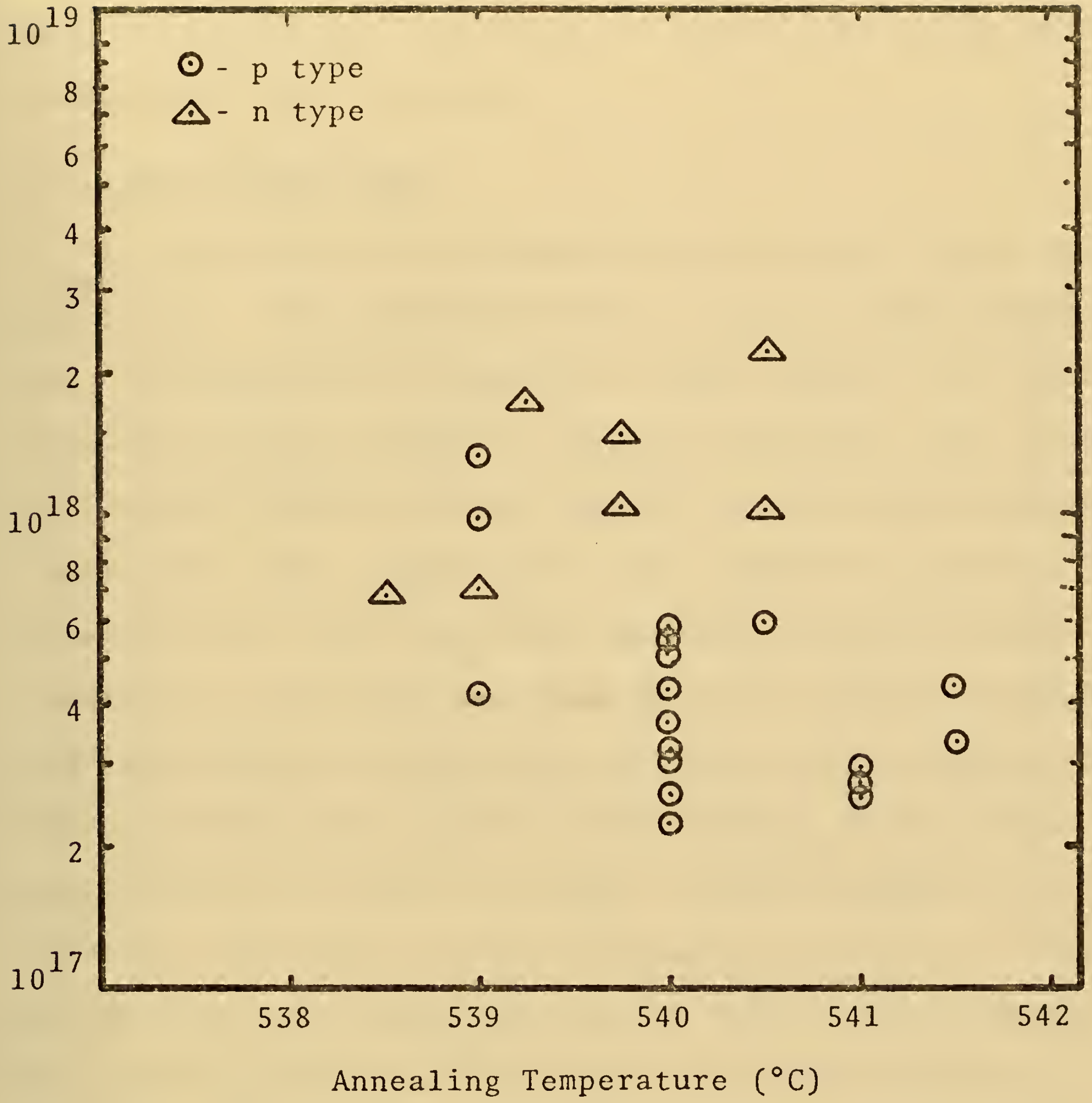

Figure 23
Concentration vs. temperature as a result of isothermal annealing

Even though the carrier type or concentration was not exactly reproducible, samples were consistently annealed with concentrations in the low to mid $10^{17}/cm^2$ which were adequate for this research.

B. PROTON BOMBARDMENT

As the samples were prepared they fell into three broad categories. They included those that were n-type throughout the investigated temperature range (Figure 24), those that were p-type through the range (Figure 25), and those that showed a Hall reversal somewhere in the investigated temperature range (Figure 21). The samples of greatest interest were those exhibiting the Hall reversal characteristics. The reason was that the Hall reversal samples had hole carrier concentrations closer to the electron carrier concentrations and thus would undergo carrier type conversion more easily. The Hall reversal samples were used for bombardment studies although one or two of each of the others was bombarded for the sake of completeness. The results of proton bombardment are shown in Tables II, III, and IV, and examples of the resulting electrical properties are shown in Figures 26 through 29.

Proton dosages of $2 \times 10^{13}/cm^2$ were initially attempted and were raised during the course of this research to a maximum of $1 \times 10^{16}/cm^2$. Dosages of $5 \times 10^{13}/cm^2$ were required to produce carrier type conversions in p-type $Pb_{0.76}Sn_{0.24}Te$ samples (see Table II). These results

TABLE II

RESULTS OF PROTON BOMBARDMENT ON $Pb_{0.76}Sn_{0.24}Te$

Sample Number	Thickness (microns)	Accumulated Dose (p/cm^2)	Carrier Concentration at 90°K (per cm^3)	Mobility at 90°K (cm^2/v-sec)	Hall Reverse Temperature (°K)
24-2	2.58	Before	1.50×10^{17} (p)	3525	248
		5×10^{13}	2.33×10^{17} (n)	1590	-

TABLE III

RESULTS OF PROTON BOMBARDMENT ON p-type $Pb_{0.80}Sn_{0.20}Te$

Sample Number	Thickness (microns)	Accumulated Dose (p/cm^2)	Carrier Concentration at 90°K (per cm^3)	Mobility at 90°K (cm^2.V-sec)	Hall Reverse Temperature (°K)
11	1.08	Before	3.50×10^{17} (p)	1000	-
		5×10^{13}	5.96×10^{17} (p)	930	-
		1.05×10^{15}	4.39×10^{17} (p)	500	320
12	1.15	Before	3.26×10^{17} (p)	400	287
		5×10^{13}	4.20×10^{17} (p)	640	-
		1.05×10^{15}	3.71×10^{17} (p)	160	271
13	1.21	Before	2.95×10^{17} (p)	520	-
		5×10^{13}	4.39×10^{17} (p)	480	-
		1.05×10^{15}	3.60×10^{17} (p)	270	321
15	1.68	Before	2.94×10^{17} (p)	1200	273
		5×10^{13}	3.97×10^{17} (p)	1100	-
		1.05×10^{15}	2.48×10^{17} (p)	830	299
32	2.56	Before	8.97×10^{17} (p)	550	152
		5×10^{13}	3.02×10^{17} (p)	650	285
		1.05×10^{15}	2.66×10^{17} (p)	500	272
38	2.50	Before	2.16×10^{17} (p)	440	285
		2×10^{14}	1.67×10^{17} (p)	470	-

TABLE III (continued)

Sample Number	Thickness (microns)	Accumulated Dose (p/cm^2)	Carrier Concentration at 90°K (per cm^3)	Mobility at 90°K (cm^2/V-sec)	Hall Reverse Temperature (°K)
40	2.81	Before	3.50×10^{17} (p)	2500	-
		2×10^{14}	3.05×10^{17} (p)	860	327
46	1.01	Before	2.42×10^{18} (p)	800	258
		2×10^{14}	5.21×10^{18} (p)	80	186
		4.4×10^{14}	4.66×10^{18} (p)	150	214
		5.44×10^{15}	4.12×10^{17} (n)	570	-
47	0.94	Before	3.01×10^{17} (p)	170	270
		2×10^{14}	2.92×10^{17} (p)	1400	171
		4×10^{14}	2.87×10^{17} (p)	1200	140
		5.4×10^{15}	2.58×10^{16} (n)	1700	-
77	1.57	Before	4.59×10^{17} (p)	11000	-
		5×10^{15}	1.93×10^{17} (p)	3900	-
82	1.51	Before	4.21×10^{17} (p)	410	285
		4.8×10^{15}	3.24×10^{17} (p)	110	216

TABLE IV

RESULTS OF PROTON BOMBARDMENT ON n-type $Pb_{0.80}Sn_{0.20}Te$

Sample Number	Thickness (microns)	Accumulated Dose (p/cm^2)	Carrier Concentration at 90°K (per cm^3)	Mobility at 90°K (cm^2/V-sec)	Hall Reverse Temperature (°K)
62	2.42	Before	4.64×10^{17} (n)	11000	-
		2×10^{15}	2.91×10^{17} (n)	3900	-
78	1.66	Before	1.22×10^{18} (n)	3500	-
		1×10^{16}	1.36×10^{16} (n)	5900	-

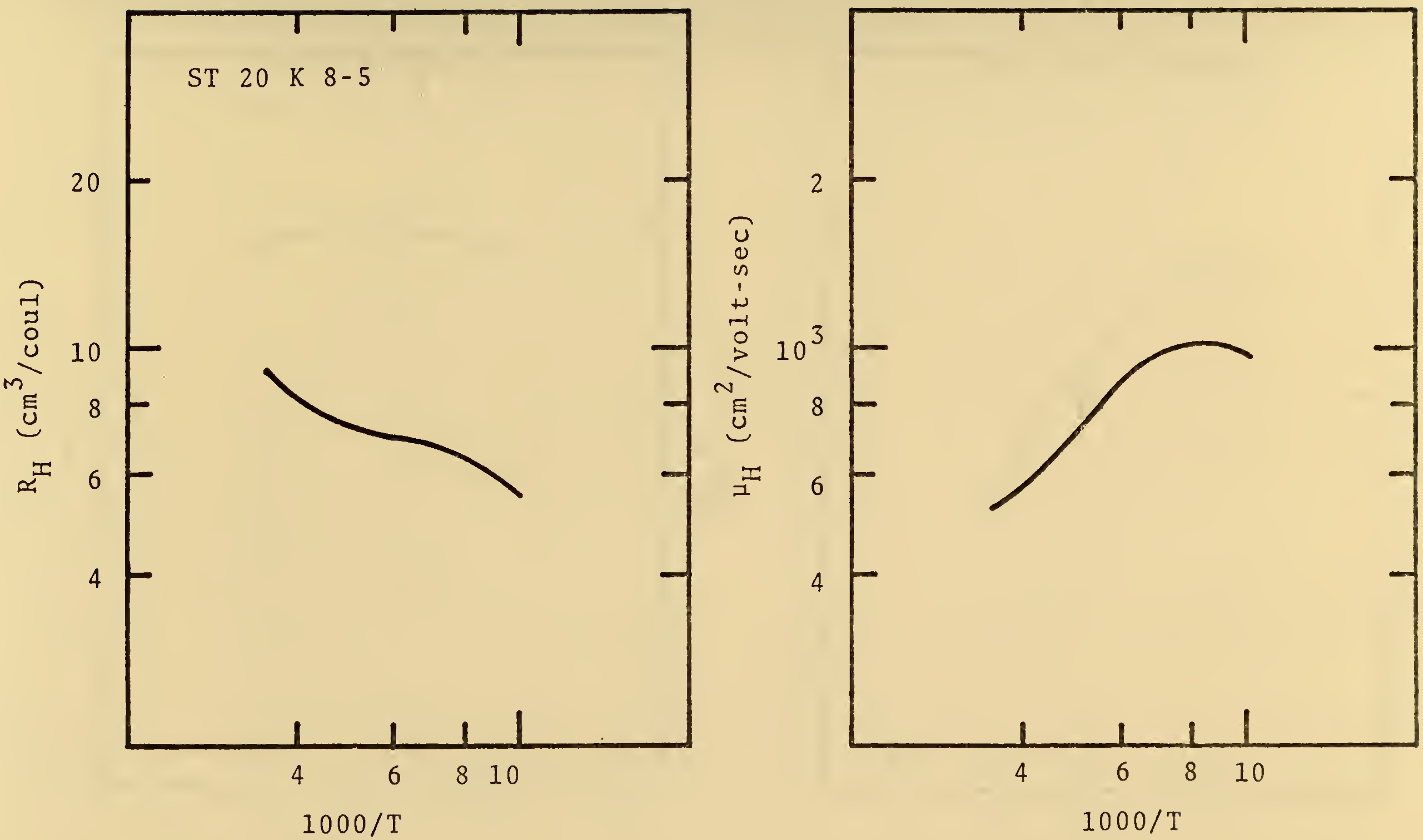

Figure 24

The Electrical Properties of a Typical n-Type Sample with No Hall Reversal

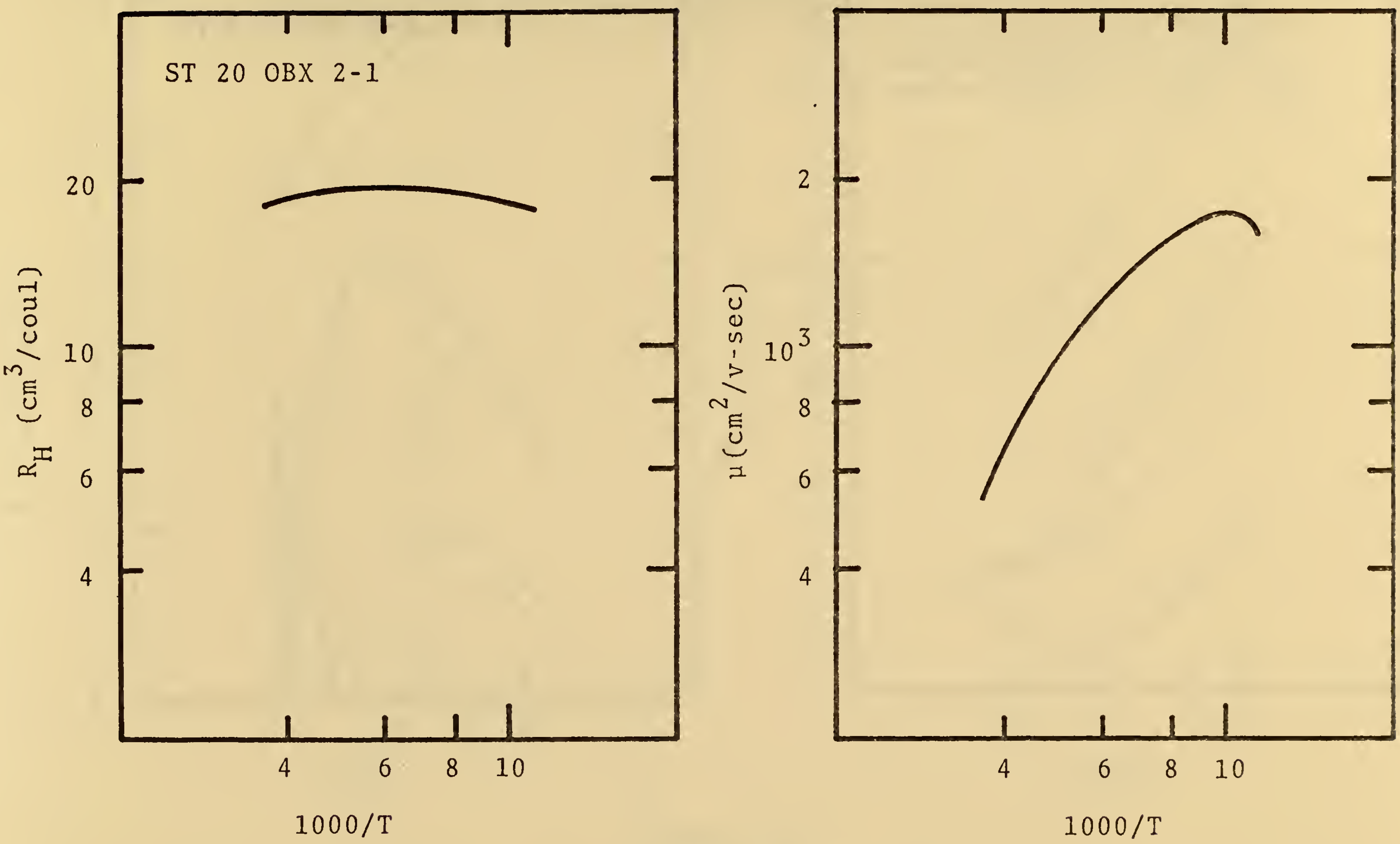

Figure 25

The Electrical Properties of a Typical
p-type Sample with No Hall Reversal

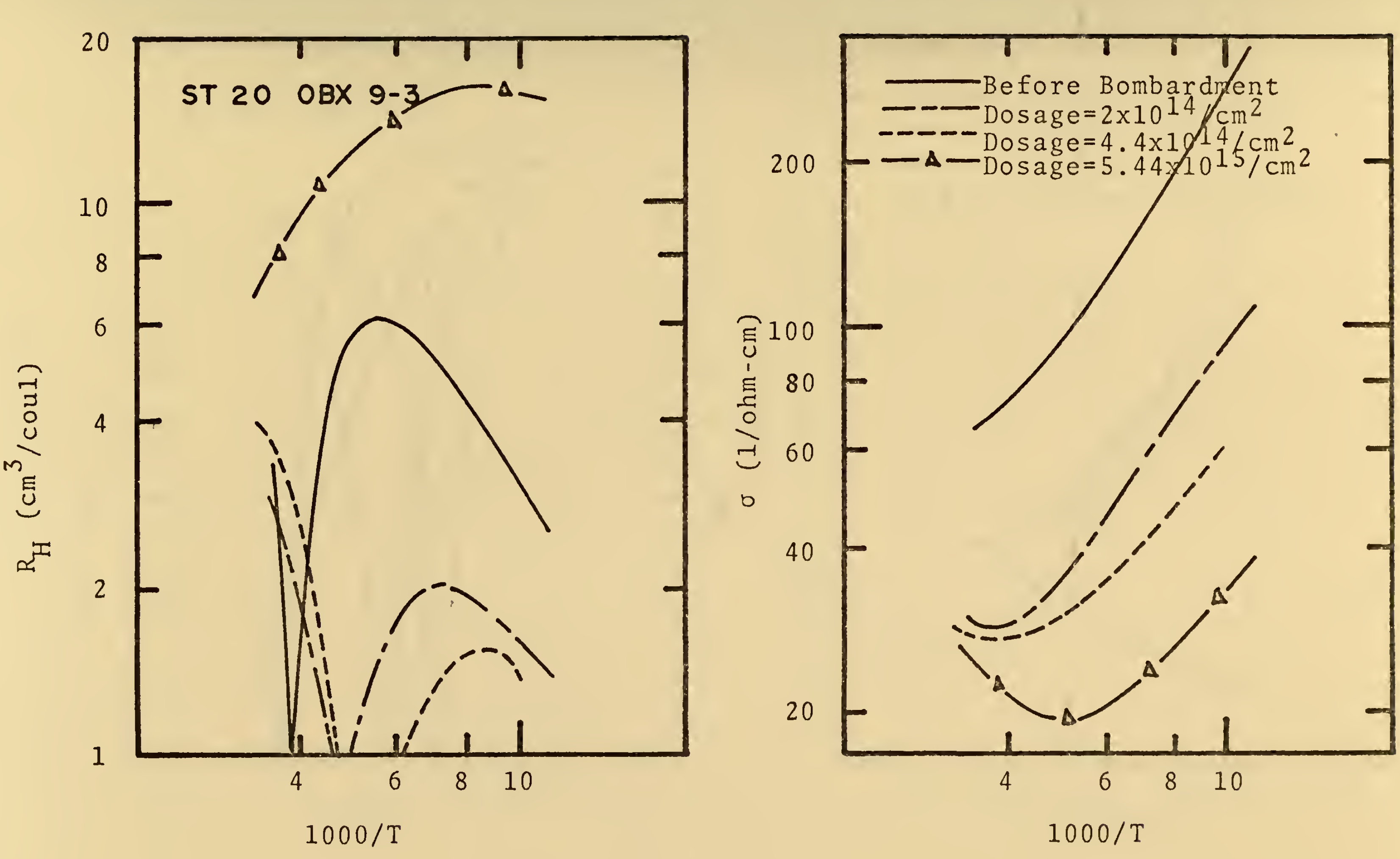

Figure 26

Electrical Properties of Sample #46 Showing
Progression as a Result of Proton Bombardment

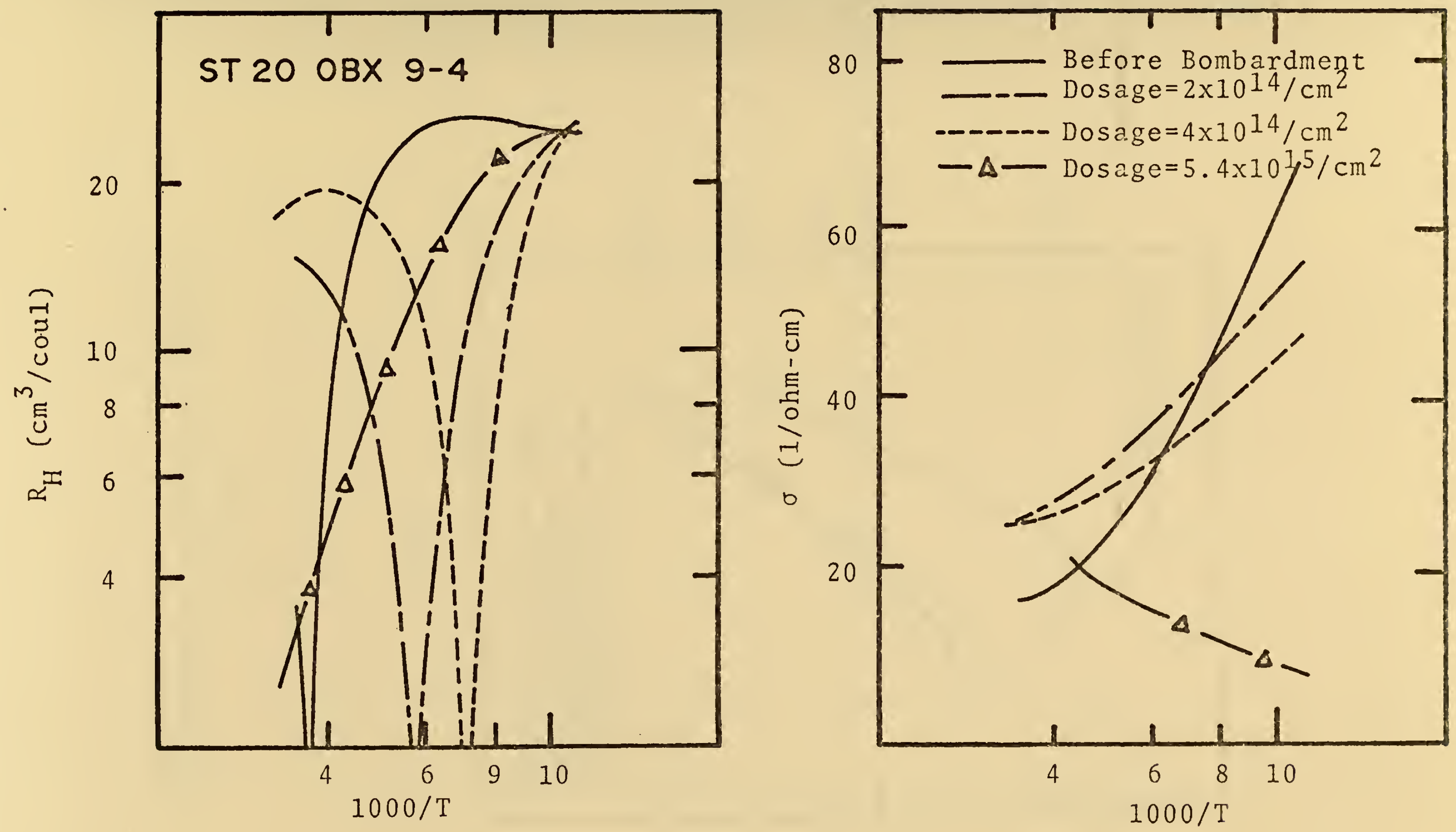

Figure 27

Electrical Properties of Sample #47 Showing Progression as a Result of Proton Bombardment

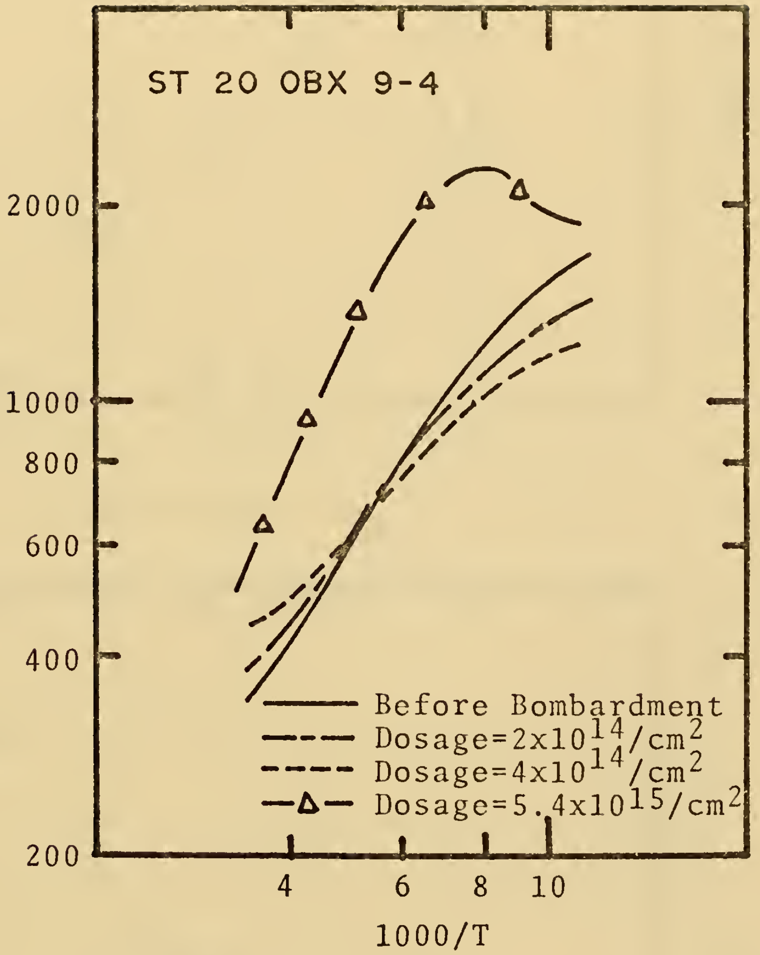

Figure 28

Mobility Variation of Sample #47
as a Result of Proton Bombardment

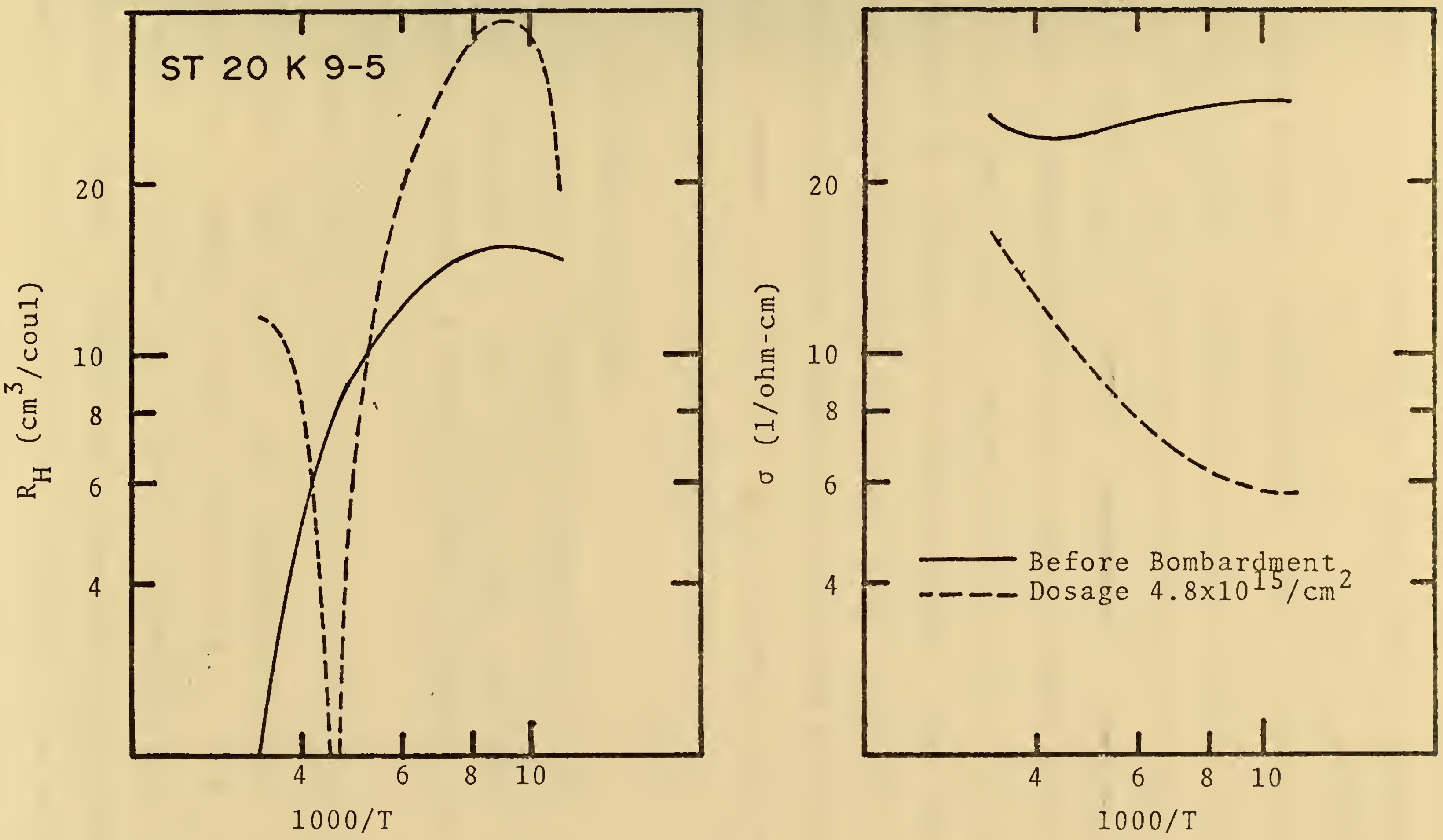

Figure 29

Electrical Properties of Sample #82 before and after Bombardment

substantial previous research [Ref. 40]. The electrical properties of the 24% samples after proton bombardment were also as expected. $Pb_{0.80}Sn_{0.20}Te$ samples (see Table III) required dosages in excess of 5 x 10^{15} to produce carrier type conversion. Progressively larger dosages starting from 2 x $10^{13}/cm^2$ up to the required conversion dosage provided small reductions in carrier concentration, reductions in mobility and lowering of Hall reversal temperatures. Mobilities and carrier concentrations after conversion appeared to follow no particular pattern. The two n-type samples that were bombarded (see Table IV) showed decreased mobility at the lower dosages and increased mobility at the higher dosages. The mobility versus dosage relationship is inconclusive due to insufficient data.

C. ISOCHRONAL ANNEALING

The results of isochronal annealing for a $Pb_{0.76}Sn_{0.24}Te$ sample are shown in Figure 30 and were consistent with previous research. A smooth recovery occurred after isochronal annealing at 105°C.

Because the Hall coefficient of the $Pb_{0.80}Sn_{0.20}Te$ samples was still varying with temperature in the low temperature ranges, the Hall coefficient at 90°K could not be used to describe the isochronal annealing effects. Instead, the Hall coefficient curves after each stage of isochronal annealing when plotted together can more graphically present the progression of isochronal annealing

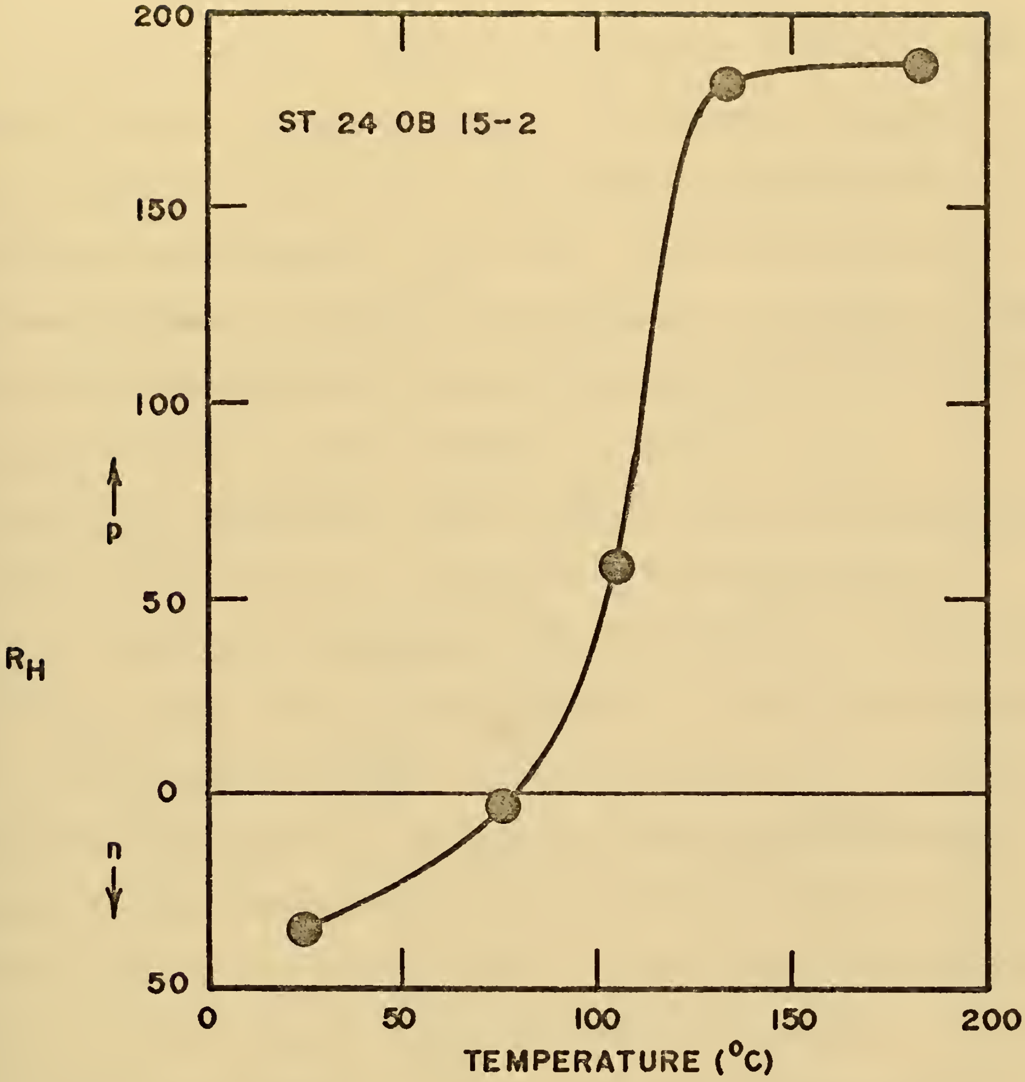

Figure 30

Results of Isochronal Annealing (24% Sample)

changes. Figures 31 and 32 present the effects of isochronal annealing on samples #46 and #47, respectively.

During the initial stages of isochronal annealing the bombarded samples remained n-type but did show a shift toward intrinsic conduction. The lowest concentration reached was approximately 1.8 x 10^{16}. As the annealing progressed further, recovery occurred and the samples became p-type and exhibited Hall reversal characteristics. Recovery temperatures were in the vicinity of 140°C.

One of the bombarded n-type samples was also subjected to isochronal annealing. The results are displayed in Figure 33 showing an unexpected shift to p-type. Since the sample was n-type prior to bombardment, it was not expected that it would exhibit p-type characteristics as a result of isochronal annealing. It is possible that the vacancies produced by the bombardment were filled as a result of isochronal annealing around 140°C by ions which behaved as acceptors. The thermal energy at 140°C is 0.0352 eV so it is assumed that 0.0352 eV is near the activation energy associated with the bombardment induced defects. Further pursuit of this phenomena should be a good subject for additional research.

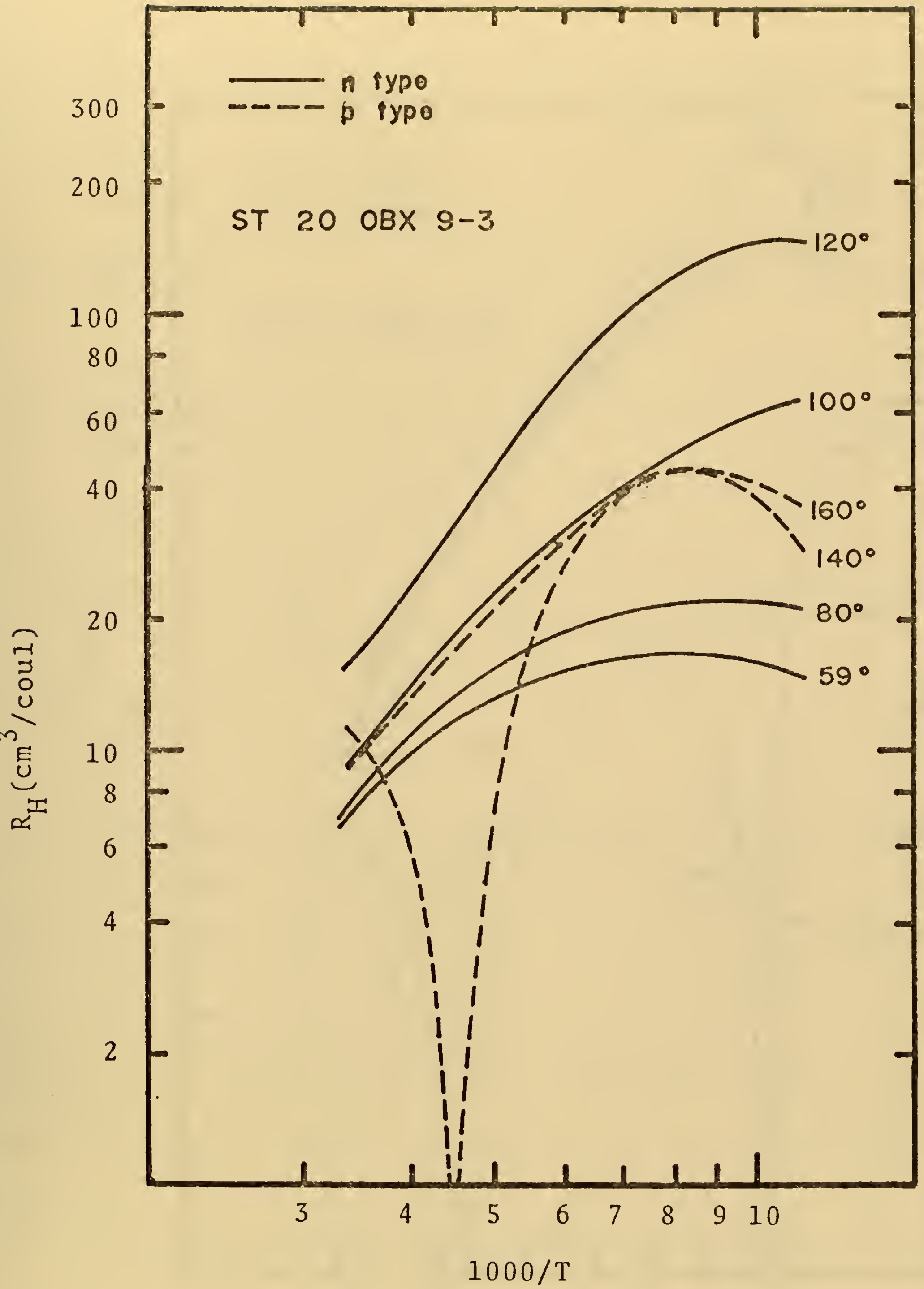

Figure 31

Results of Isochronal Annealing (Sample #46)

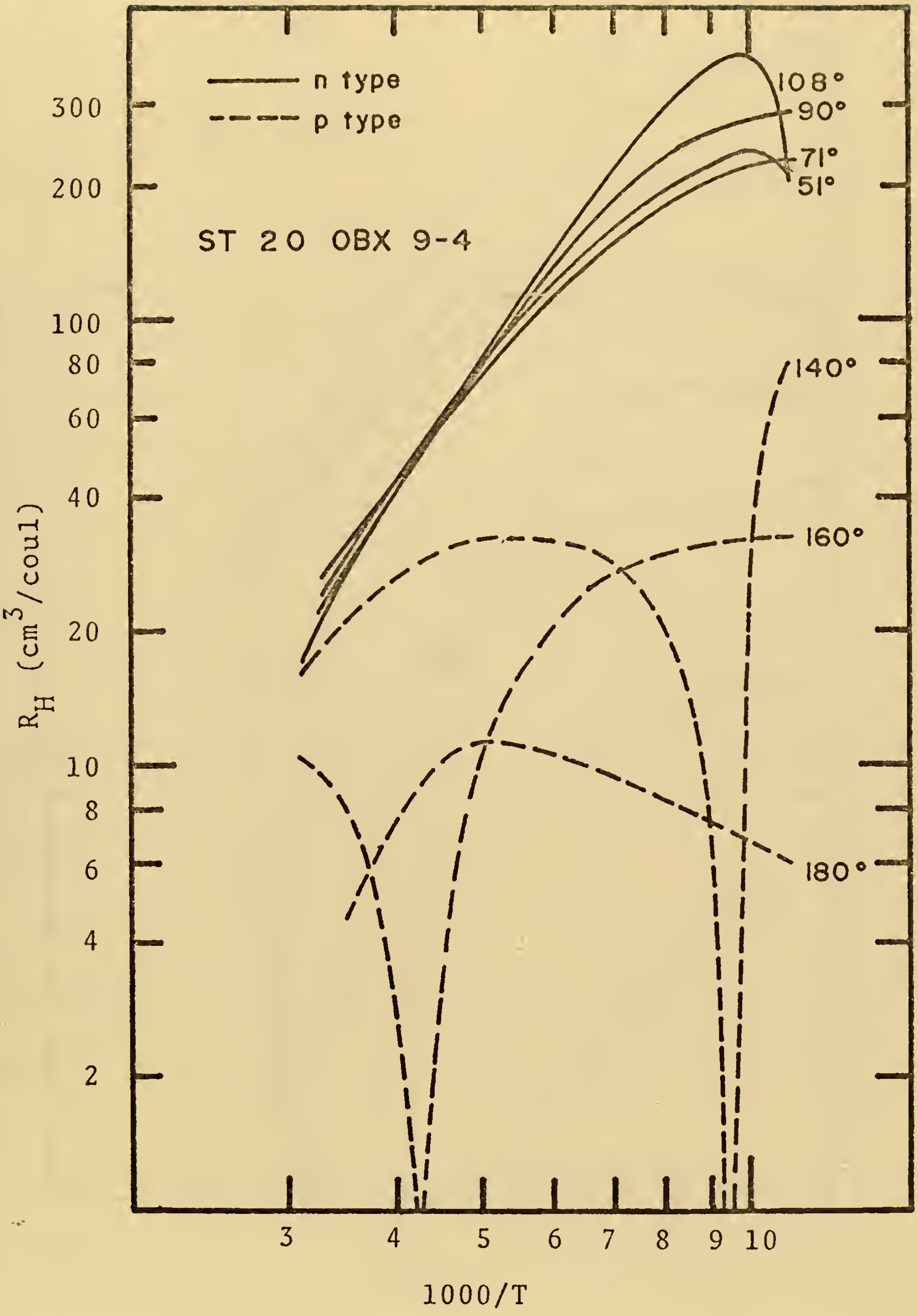

Figure 32
Results of Isochronal Annealing (Sample #47)

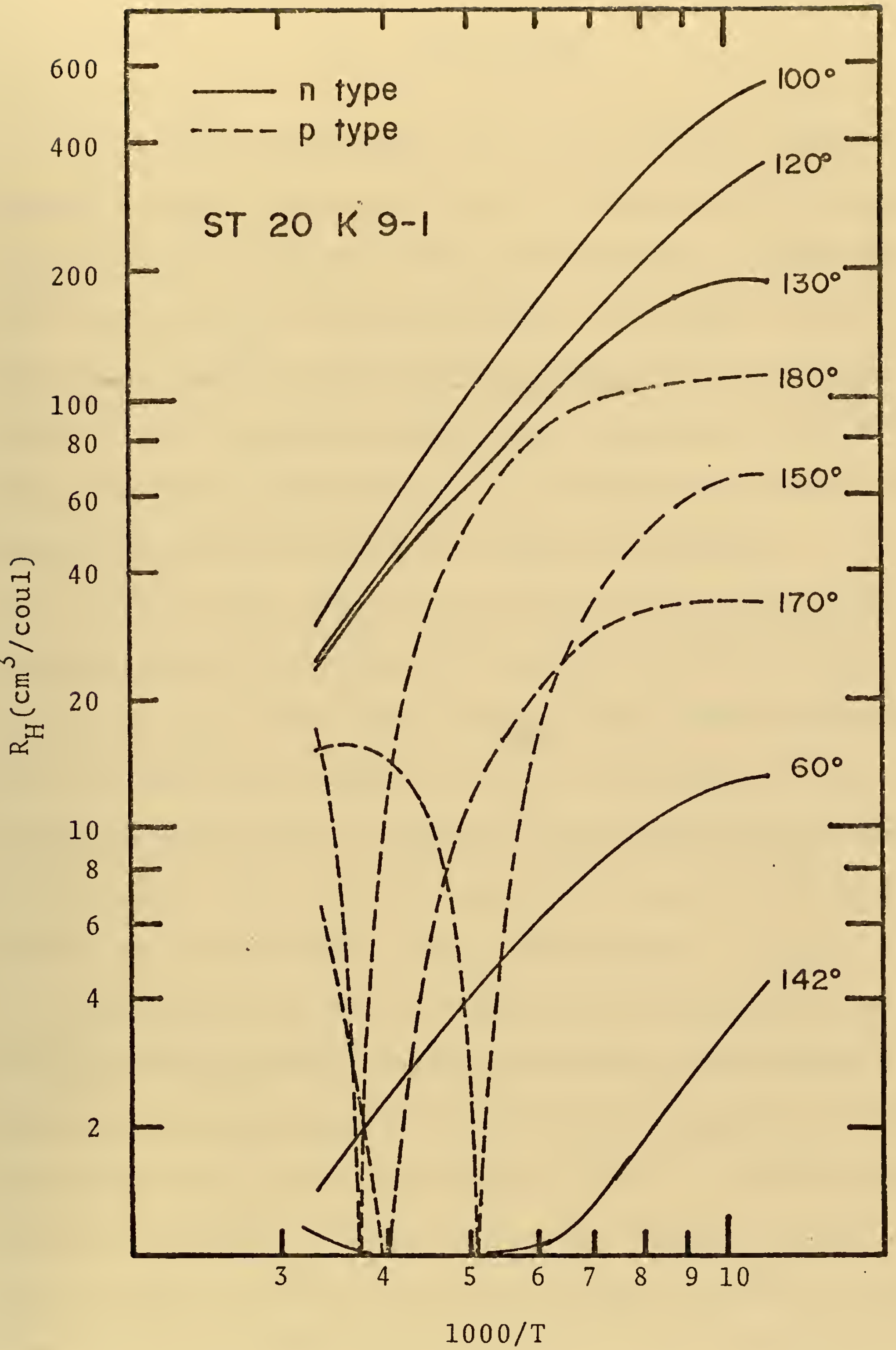

Figure 33
Results of Isochronal Annealing (n-type sample)

IV. CONCLUSIONS

Isothermal annealing can be successfully employed to reduce carrier concentrations and change carrier type in the materials studied. The stoichiometric temperature, T_o, for $Pb_{0.80}Sn_{0.20}Te$ was determined to be approximately 540°C. Thin film samples with carrier concentrations in the low to mid $10^{17}/cm^3$ could be consistently produced. It is felt that isothermal annealing has no significant effect on the mobilities of the thin film samples involved.

Carrier type conversion of p-type $Pb_{0.80}Sn_{0.20}Te$ can be accomplished by bombardment with 200-250KeV protons. Dosages in excess of $5 \times 10^{15}/cm^2$ are required, much higher than the $5 \times 10^{13}/cm^2$ required for $Pb_{0.76}Sn_{0.24}Te$. Lower dosages provided reductions in carrier concentrations and reductions in mobility. The carrier concentrations and mobilities after conversion could not be predicted.

The effects of proton bombardment appeared to be stable at room temperature; however, no long-term study was made. Isochronal annealing revealed that the recovery temperatures for converted p-type samples to return to n-type were in the vicinity of 140°C. Bombarded n-type samples showed significant changes of their electrical properties near this temperature as well as an unexpected conversion to p-type. The activation energy of bombardment induced defects of this nature seems to be about 0.035 eV.

Proton bombardment has shown promise in fabricating photovoltaic diode arrays on InSb, PbTe and $Pb_{0.88}Sn_{0.12}Te$ materials in the past two years. This research has demonstrated that the same technique can convert $Pb_{1-x}Sn_xTe$ of higher Sn contents also. However, based on the isochronal annealing study, it is found that the effect of proton bombardment can be drastically changed by moderate heating at temperatures as low as 140°C. This discovery leads to the suspicion that the long-term stability is poor.

Further investigation is recommended of the isothermal annealing method and the determination of the exact stoichiometric temperature, T_o, for $Pb_{0.80}Sn_{0.20}Te$. The establishment of T_o is important in the preparation of materials with uniform characteristics for proton bombardment.

It is strongly recommended that the mechanisms of conversion be thoroughly studied. In addition, investigation of the use of different species of high energy particles for bombardment as well as various crystal orientations and temperatures during bombardment should be studied to determine the best conditions for bombardment and long-term stability. The question of stability should be extensively pursued. Methods of raising the activation energy of bombardment induced defects must be investigated before useful devices can be fabricated.

COMPUTER PROGRAM FOR THE DETERMINATION OF CARRIER CONCENTRATIONS AND MOBILITIES IN PB SN TE

```
      DATA IS STARTED FROM THE LOWEST TEMPERATURE


      D=THICKNESS IN MICRONS
      B=MOBILITY RATIO MUN/MUP
      BO=MOBILITY RATIO AT HALL REVERSAL TEMPERATURE
      BO=VC(EXT)/VC(EXT)-VC(0)
      EG=ENERGY GAP IN EV
      EGO=ENERGY GAP AT 0 DEGREES KELVIN
      T=TEMPERATURE IN DEGREES KELVIN
      TO=TEMPERATURE AT HALL REVERSAL IN DEGREES KELVIN
      VH=HALL VOLTAGE IN MV
      VH IS POSITIVE FOR P-TYPE, NEGATIVE FOR N-TYPE
      VC=CONDUCTIVITY VOLTAGE IN MV
      XII=NUMBER OF DATA CARDS
      PE=P-N
      Z=WAVELENGTH IN MICRON


      PROGRAM STARTS

      DIMENSION VH(30),VC(30),T(30),R(30),T1(30),C(30),Z(30)
     1HH(30)
      XM=9.107E-28
      H=6.625E-27
      XK=1.380E-16
      Q=1.600E-19
    5 READ(5,105,END=999) D,BO,EGO,TO,XII
  105 FORMAT(8F10.2)
      PRINT 101
      IF(D.LE.0.) GO TO 999
      PE=0.
      GAMA=0.0
      IM=XII
   10 READ(5,175)(VH(I),VC(I),T(I),I=1,IM)
  175 FORMAT(3F10.2)
C
C             CALCULATE THE HALL COEFFICIENT AND CONDUCTIVITY
C
C     0.5 IS FOR MAGNETIC FIELD = 0.5 WEBER/M**2
C     26900 IS FOR HALL SAMPLE
C     SAMPLE CURRENT IS 1 MA
C     EG(T)=EG(0)+4.6*10-4*T FOR PB SN TE
  200 DO 300 I=1,IM
      EG(I)=EGO+4.6E-4*T(I)
      Z(I)=6.625*0.3/(1.6*EG(I))
C     0.85 IS A FACTOR TO CORRECT FOR THICKNESS
      R(I)=0.85*VH(I)*2.0*D
      C(I)=26900.0/(VC(I)*0.85*D)
      T1(I)=1000.0/T(I)
      IF (PE.LE.0.) PE=1./(R(I)*Q)
C
C             CALCULATE THE CARRIER CONCENTRATIONS, N, P, NI
C
C     HE=1
C     HH=0.89 AT 90 DEG INCREASING TO 1.0 AT 200 DEG
C     HH=1.0 BEYOND 200 DEG
      HH(I)=1.
      IF(T(I).LT.90.0) T(I)=90.
  300 IF(T(I).LT.200.) HH(I)=0.89+0.001*(T(I)-90.)
   32 PRINT 102,GAMA
      DO 310 I=1,IM
      IF(R(I).EQ.0.) XN=HH(I)*PE/(BO**2-HH(I))
      IF(R(I).EQ.0.) GO TO 30
      B=BO*(T(I)/TO)**GAMA
```

```
      XB2=2*R(I)*Q*PE*(B+1.)+B**2-HH(I)
      AC=4*R(I)*Q*(B+1.)**2*(R(I)*Q*PE*PE-HH(I)*PE)
      AC=XB2**2-AC
      IF(AC.LT.0.) PRINT 110,R(I),C(I),T(I),GAMA,I
      IF(AC.LT.0.) GO TO 310
  110 FORMAT(1H0,40X,'P CAN NOT BE FOUND,R=',F10.2,'   SIGMA=
     1'  T1=',F8.2,'   GAMMA=',F5.1,'   I=',I2)
      AC=SQRT(AC)
      XN=(-XB2+AC)/(2*R(I)*Q*(B+1.)**2)
   30 P=PE+XN
      YN=XN
      XN=ABS(XN)
      XNI=SQRT(XN*P)
C
C            CALCULATE THE MOBILITIES
C
      XMUP=C(I)/(Q*(XN*B+P))
      XMUN=B*XMUP
C
C            CALCULATE THE DENSITY STATE EFFECTIVE MASS
C
      XT=-EG(I)*1.6E-12/(6.*XK*T(I))
      XT=EXP(XT)*SQRT(2.*3.14159*XK*T(I))
      YT=H*(XN*P/4.)**(1./6.)
      YT=YT/XT
      XME=YT**4
      XME=XME/(XM**2)
      YME=SQRT(XME)
      PRINT 120,T(I),T1(I),YME,YN,P,XNI,XMUP,XMUN,Z(I),EG(I)
     1,C(I),B
  120 FORMAT(1X,2F8.2,F8.3,3E12.4,2F10.2,2F8.4,F8.3,3F7.2)
  101 FORMAT(1H1,7X,'T   1000/T',2X,'     M*',11X,'N',11X,'P',
     112X,'NI',7X,'MUP',7X,'MUN   MICRON       EG    ME*MH',5X,
     2'R',2X,'SIGMA',4X,'B'//)
  102 FORMAT(1H0,1X,' GAMMA=',F5.2)
  310 CONTINUE
      GAMA=GAMA-0.25
      IF(GAMA.GE.-3.) GO TO 32
      GO TO 5
  999 PRINT 123
  123 FORMAT(1H1,'FINIS')
      STOP
      END
```

BIBLIOGRAPHY

1. Altman, L., "Optoelectronics Engineers Pit Lasers against Air Pollution," Electronics, v. 44, p. 64-68, 6 Dec 1971.

2. Butler, J. F., Calawa, A. R., and Harman, T. C., "Diode Laser of $Pb_{1-y}Sn_yTe$ and $Pb_{1-x}Sn_xTe$," Appl. Phys. Ltrs., v. 9, p. 427-429, 15 Dec 1966.

3. Butler, J. F., and Harman, T. C., "Long-wavelength Infrared $Pb_{1-x}Sn_xTe$ Diode Lasers," Appl. Phys. Ltrs, v.12, p. 347-349, 15 May 1968.

4. Strauss, A. J., "Inversion of Conduction and Valence Bands in $Pb_{1-x}Sn_xTe$ Alloys," Phys. Rev., v. 157, p. 608-611, May 1967.

5. Harman, T. C., and others, "Temperature and Composition Dependence of Laser Emission," Appl. Phys. Ltrs., v. 14, p. 333-334, 1 June 1969.

6. Melngailis, I., and Harman, T. C., Semiconductors and Semimetals, v. 5, p. 115, Academic Press, 1970.

7. Dimmock, J. O., Melngailis, I., and Strauss, A. J., "Band Structure and Laser Action in $Pb_{1-x}Sn_xTe$," Phys. Rev. Letters, v. 16, p. 1193-1196, 27 June 1966.

8. Butler, J. F., and Calawa, A. R., Physics of Quantum Electronics, p. 458-466, McGraw-Hill, 1966.

9. Nikolic, P. M., "Optical Energy Gaps, Lattice Parameters and Solubility Limits of Solid Solutions of SnSe and GeSe in PbTe and GeSe in SnTe," Brit. J. Appl. Phys., v. 16, p. 1075-1079, Aug 1965.

10. Bylander, E. G., "Reproducible Preparations of $Pb_{1-x}Sn_xTe$ Epitaxial Films with Moderate Carrier Concentrations," Mater. Sci. Eng., v. 1, p. 190-194, Sep 1966.

11. Esaki, I., and Stiles, P. J., "New Type of Negative Resistance in Barrier Tunnelling," Phys. Rev. Letters, v. 16, p.1108-1111, 13 Jun 1966.

12. Calawa, A. R., and others, "Crystal Growth, Annealing and Diffusion of Lead-Tin Chalcogenides," Trans AIME, v. 242, p. 374-383, March 1968.

13. Wagner, J. W., and Willardson, R. K., "Growth and Characterization of Single Crystals of PbTe-SnTe," Trans. AIME, v. 242, p. 366-371, March, 1968.

14. Rolls, W., Lee, R., and Eddington, R. J., "Preparation and Properties of $Pb_{1-x}Sn_xTe$ Epitaxial Films," J. Vac. Science and Tech., v. 7, p. 121-126, 1970.

15. Rolls, W., Lee, R., and Eddington, R. J., "Preparation and Properties of PbSnTe Photodiodes," Solid State Electronics, v. 13, p. 75-81, 1970.

16. Thompson, A. G., and Wagner, J. W., "Growth and Characterization of Lead-Tin Telluride Epitaxial Layers," Phys. Stat. Soli. (A), v. 5, p. 439-448, 1971.

17. Longo, J. T., Gertner, E. R., and Joseph A. S., "Low Carrier Concentration Liquid Phase Epitaxy PbSnTe," Appl. Phys. Ltrs., v. 19, p. 202-203, 1971.

18. Tao, T. F., Wang, C. C., and Sunier, J. W., "Effects of Proton Bombardment of $Pb_{0.80}Sn_{0.20}Te$," Appl. Phys. Ltrs., v. 20, p. 235-237, 1 April 1972.

19. Foyt, A. G., Harman, T. C., and Donnelly, J. P., "Type Conversion and n-p Junction Formation in $Hg_{1-x}Cd_xTe$ Produced by Proton Bombardment," Appl. Phys. Ltrs., v. 18, p. 321-323, 1971.

20. Donnelly, J. P., Harman, T. C., and Foyt, A. G., "n-p Junction Photovoltaic Detectors in PbTe Produced by Proton Bombardment," Appl. Phys. Ltrs., v. 18, p. 259-261, 1971.

21. Donnelly, J. P., Harman, T. C., and Foyt, A. G., Solid State Research Report, Lincoln Laboratory, MIT, v. 1, 1971.

22. Donnelly, J. P., Calawa, A. R., Foyt, A. G., and Lindley, W. T., "$Pb_{1-x}Sn_xTe$ Photovoltaic Diodes and Diode Lasers Produced by Proton Bombardment," Solid State Electronics, v. 15, p. 403-407, 1972.

23. Shannon, J. M., Stephen, J., and Freeman, J. H., "MOS Frequency Soars with Ion Implanted Layers," Electronics, p. 96-100, 3 Feb 1969.

24. Macdougall, J., and Manchester, K., "Ion Implantation Offers a Bagful of Benefits for MOS," Electronics, p. 86-90, 22 June 1970.

25. Crawford, B., "Implanted Depletion Loads Boost MOS Array Performance," Electronics, p. 85-90, 24 April 1972.

26. Thompson, S. A., "Ion Implantation, the Sock-it-to'em Method to Dope Semiconductors," The Electronic Engineer, p. 68-76, Jan 1969.

27. Thomsett, M. F., "Charge Transfer Devices," Bell Laboratories, To be published.

28. Mayer, J. W., and Marsh, O. J., Applied Solid State Science, v. 1, p. 240, Academic Press, 1969.

29. Donelly, J. P., and others, "Type Conversion and p-n Junctions in n-CdTe Produced by Ion Implantation," Appl. Phys. Ltrs., v. 12, p. 303-305, 1968.

30. Anderson, W. W., and Mitchell, J. T., "Phosphorous-Ion Implanted CdS," Appl. Phys. Ltrs., v. 12, p. 334-336, 1968.

31. Chernow, F., and others, "High Conductivity p-type CdS," Appl. Phys. Ltrs., v. 12, p. 339-341, 1968.

32. Donnelly, J. P., and others," PbTe Photodiodes Fabricated by Sb^+ Ion Implantation," Conference on the Physics of IV-VI Compounds and Alloys, Philadelphia, Penn., 24-25 March 1972.

33. Dunlap, H., and others, "Development of Ion Implantation Techniques for Micro-electronics," Quart. Prog. Rept. No. 4, Contract NAS 12-124, Hughes Res. Lab., 1967.

34. Leith, F. A., King, W. J. and McNally, P., "High Energy Ion Implantation of Materials," Final Report Contract AF 9 (628)-4970, 1967.

35. Roughan, P. E., and Manchester, K. E., "Properties of Ion Implanted GaAs Diodes," J. Electrochem Soc., v. 16, p. 278-279, 1969.

36. Hunsperger, R., Marsh, O. J., and Mead, C., "The Presence of Deep Levels in Ion Implanted Junctions," Appl. Phys. Ltrs., v. 13, p. 295-297, 1968.

37. Mayer, J. W., and others, "Nz and Te Implantations into GaAs," Appl. Phys. Ltrs., v. 38, p. 1975-1976, 1967.

38. Foyt, W. T., Lindley, W. T. and Donnelly, J. P., "n-p Junction Photodetectors in InSb Fabricated by Proton Bombardment," Appl. Phys. Ltrs., v. 16, p. 335-337, 1970.

39. Bis, A. F., and Dixon, J., "Single-Crystal Films of $Pb_{1-x}Sn_xTe$ Alloys," Bull. Am. Phys. Soc., v. 12, p. 327, March 1967.

40. Wang, C. C., Properties of Thin Film Lead-tin Telluride and Lead-Ten Selenide Infrared Photoconductors, Ph.D. Thesis, UCLA, 1971.

41. Brebrick, F. F. and Algaier, R. S., "Composition Limits of Stability of PbTe," J. Chem. Phys., v. 32, p. 1826-1831, June 1960.

42. Smith, R. A., Semiconductors, p. 123, University Press, 1964.

INITIAL DISTRIBUTION LIST

		No. Copies
1.	Defense Documentation Center Cameron Station Alexandria, Virginia 22314	2
2.	Library, Code 0212 Naval Postgraduate School Monterey, California 93940	2
3.	Assoc. Professor T. F. Tao, Code 52 Department of Electrical Engineering Naval Postgraduate School Monterey, California 93940	5
4.	Dr. W. W. Scanlon Chief, Department of Applied Physics Naval Ordnance Laboratory White Oak, Silver Spring, Maryland 20910	1
5.	Mr. Richard Schoolar Department of Applied Physics Naval Ordnance Laboratory White Oak, Silver Spring, Maryland 20910	1
6.	Dr. Donald Simons Department of Applied Physics Naval Ordnance Laboratory White Oak, Silver Spring, Maryland 20910	1
7.	Mr. R. Hickmott AFML/LPE Air Force Materials Laboratory Wright-Patterson Air Force Base, Ohio 45433	2
8.	LT David G. Anderson, USN Class #41 Naval Destroyer School Newport, Rhode Island 02840	1

DOCUMENT CONTROL DATA - R & D

(Security classification of title, body of abstract and indexing annotation must be entered when the overall report is classified)

ORIGINATING ACTIVITY (Corporate author) Naval Postgraduate School Monterey, California 93940	2a. REPORT SECURITY CLASSIFICATION Unclassified 2b. GROUP

REPORT TITLE

The Effects of Proton Bombardment on PbSnTe

DESCRIPTIVE NOTES (Type of report and, inclusive dates)

Master's Thesis, December 1972

AUTHOR(S) (First name, middle initial, last name)

David Graham Anderson

REPORT DATE December 1972	7a. TOTAL NO. OF PAGES 86	7b. NO. OF REFS 42
. CONTRACT OR GRANT NO.	9a. ORIGINATOR'S REPORT NUMBER(S)	
. PROJECT NO.		
.	9b. OTHER REPORT NO(S) (Any other numbers that may be assigned this report)	
.		

. DISTRIBUTION STATEMENT

Approved for public release; distribution unlimited

. SUPPLEMENTARY NOTES	12. SPONSORING MILITARY ACTIVITY Naval Postgraduate School Monterey, California 93940

. ABSTRACT

The effects of 200-250 KeV proton bombardment on both p-type and n-type $Pb_{0.80}Sn_{0.20}Te$ thin films were investigated. Emphasis was placed on p-type samples to determine the feasibility and dosage required to change the carrier type and to determine the stability after bombardment. This method of conversion has promise in the fabrication of photovoltaic diode arrays for infrared applications. The samples were characterized by Hall effect and conductivity measurements from 90°K to 300°K. It was found that p-type $Pb_{0.80}Sn_{0.20}Te$ samples of initial concentrations in the low to mid $10^{17}/cm^3$ range can be converted to n-type with dosages above 5×10^{15} p/cm^2, considerably higher than the low to mid 10^{13} p/cm^2 needed to convert $Pb_{1-x}Sn_xTe$ of other Sn contents. Stability was investigated using isochronal annealing methods with temperatures up to 180°C. It was found that significant changes of the proton bombardment effects occurred around 140°C. Type converted n samples were found to return to p-type at this temperature.

D FORM 1 NOV 65 1473 (PAGE 1)

N 0101-807-6811

14. KEY WORDS	LINK A		LINK B		LINK C	
	ROLE	WT	ROLE	WT	ROLE	WT
Proton Bombardment						
PbSnTe						
Infrared detectors						
Lead-Tin Chalcogenides						
Lead-Tin-Telluride						

Thesis
A4456
c.1
141209
Anderson
The effects of proton
bombardment on PbSnTe.